

The Role of Meson Retardation in the NN Interaction above Pion Threshold <sup>y</sup>

Michael Schwamb and Hartmut Arenhövel

Institut für Kernphysik, Johannes Gutenberg-Universität, D-55099 Mainz, Germany

A model is developed for the hadronic interaction in the two-nucleon system above pion threshold which is based on meson, nucleon and degrees of freedom and which includes full meson retardation in the exchange operators. For technical reasons, the model allows maximum alone meson to be present explicitly. Thus the Hilbert space contains besides  $N\bar{N}$  and  $N\pi$  also configurations consisting of two nucleons and one meson. For this reason, only two- and three-body unitarity is obeyed, and the model is suited for reactions in the two nucleon sector only, where one pion is produced or absorbed. Starting from a realistic pure nucleonic retarded potential, which had to be renormalized because of the additional and degrees of freedom, a reasonable fit to experimental  $N\bar{N}$ -scattering data could be achieved.

## I. INTRODUCTION

At present one of the most interesting topics in the field of medium energy physics is concerned with the role of effective degrees of freedom (d.o.f.) in hadronic systems in terms of nucleon, meson and isobar d.o.f. and their connection to the underlying quark-gluon dynamics of QCD. For the study of this interesting and basic question, the two-nucleon system provides an important test laboratory, because it is obviously the simplest nuclear system for the study of the fundamental nucleon-nucleon interaction in  $N\bar{N}$  scattering including deuteron properties, and, furthermore, for testing this effective description in other reactions, for example, in elastic and inelastic electron deuteron scattering, in deuteron photodisintegration, and meson photo- and electroproduction on the deuteron. Moreover, due to the lack of free neutron targets, reactions on the deuteron are also an important tool to test our present understanding of neutron properties. As an example for the latter aspect, we would like to mention the recently much discussed determination of the electric form factor  $G_E(n)$  of the neutron in  $d(e;e'n)p$  [1] and  $d(e;e'n)p$  [2], or the investigation of the Gerasimov-Drell-Hearn sum rule for the deuteron [3]. However, in order to separate the unwanted binding effects from the neutron properties, a precise knowledge of the structure dependent effects is needed.

Intense efforts over many past decades in experiment and theory have shown that for energies below pion threshold a satisfactory description of  $N\bar{N}$  scattering and deuteron properties [4,5], as well as photo- and electrodisintegration of the deuteron is achieved within the conventional framework of nucleon, meson and isobar d.o.f. [6,7], although the description of observables is not perfect because for certain observables significant discrepancies remain unresolved as, for example, in elastic electron deuteron scattering [8]. At higher energies, above pion threshold our theoretical understanding of the various experimental data is much less well settled. Even for deuteron photodisintegration (for a detailed review see [6]), none of the various theoretical approaches like the diagrammatic method of Laget [9], the framework of nuclear isobar configurations in the impulse approximation [10], the unitary three-body model [11] or the coupled channel approach (CC) [12,13] is able to describe in a satisfactory manner the whole set of experimental results on differential cross sections and polarization observables for energies covering the whole resonance region.

A common feature of most of these approaches is the extensive use of the static limit for the meson propagator which enters the hadronic interaction and the electromagnetic two-body exchange current operators, although there is little justification for that in view of the relatively high excitation energies involved. The reason for this severe approximation is the enormous simplification of the operator structure becoming local, and thus is much simpler to evaluate numerically. It has already been conjectured in [13], that one main reason for the above mentioned failure of the theoretical description lies in the neglect of meson retardation in the meson exchange operators. Indeed, first results [14,15] based on the thesis of M. Schwamb [16] have shown that a much better description of deuteron photodisintegration compared to the static approaches is obtained if meson retardation is retained.

In the present paper, we want to lay down the foundations for future studies of the effect of meson retardation in various reactions. To this end we will set up here the basic framework of a model for the hadronic interaction in which retardation in the exchange operators is included. We would like to emphasize the fact that this formalism

---

<sup>y</sup>Supported by the Deutsche Forschungsgemeinschaft (SFB 443).

can be applied to any reaction on the two-nucleon system for excitation energies up to about 500 MeV in which not more than one pion is produced or absorbed. But in this work we will restrict ourselves to the hadronic interaction in studying  $N\bar{N}$  scattering and deuteron properties only in order to x all free hadronic parameters of our model. The application of this formalism to other hadronic reactions like  $d$  scattering as well as to electromagnetic reactions will be deferred to forthcoming papers.

The next section is devoted to the conceptual basis and the main features of our model. In view of the fact that conventional retarded interactions in pure nucleonic space are energy dependent and thus non-hermitean, we enlarge the Hilbert space by considering explicitly meson and d.o.f. in order to start with a hermitean hamiltonian. The retarded interaction is then generated by meson-nucleon and  $N\bar{N}$  vertices. For reasons of simplicity, we restrict ourselves in this work to configurations with only one meson present besides the baryons. Special attention is laid on the question of nucleon dressing and the corresponding renormalization of operators as well as the fulfillment of two- and three-body unitarity. The Lippmann-Schwinger equation for  $N\bar{N}$  scattering is derived, and the structure of the deuteron is discussed. A full theoretical realization in the form of a one-meson-exchange model is developed in Sect. III with inclusion of the isobar which is conceptually similar to the work of the Bonn group [17]. In particular, we will discuss here the important question of double counting if realistic potential models are used as input. Then we will present and discuss in Sect. IV the results for  $N\bar{N}$  scattering, where we will compare our results with experiment as well as with other theoretical approaches. Finally, Sect. V contains a summary and an outlook.

## II. BASIC CONSIDERATIONS

### A. The Hilbert space

As outlined in the introduction, our model for the description of the two-nucleon system allows besides two nucleons configurations with the additional presence of one meson or configurations where one nucleon is replaced by a isobar. It is similar (but not identical) to the approach of Sauer and collaborators [18{21] which is also used in [13,22,23]. Thus the model Hilbert space  $H^{[2]}$  is subdivided into three orthogonal spaces according to the different configurations containing either two bare nucleons ( $H_{NN}^{[2]}$ ), one nucleon and one ( $H_N^{[2]}$ ), or two nucleons and one meson ( $H_{XNN}^{[2]}$ ), i.e.

$$H^{[2]} = H_{NN}^{[2]} \quad H_N^{[2]} \quad H_{XNN}^{[2]} : \quad (1)$$

The 'bar' indicates a bare nucleon to be distinguished from the corresponding physical nucleon denoted without a bar. For the isobar we will not make this distinction, because the self energy contributions from  $N$  loops will be retained explicitly, whereas the dressing of the bare nucleon to become a physical nucleon will be incorporated in the operators by so-called dressing factors. In  $H_{XNN}^{[2]}$  only one meson is present besides two nucleons, i.e., no components with two or more mesons are taken into account (one-meson approximation). This means in detail

$$H_{XNN}^{[2]} = \begin{matrix} M \\ \times 2f ; ; ; ; ! ; g \end{matrix} \quad H_{XNN}^{[2]} : \quad (2)$$

As indicated in the direct product, we will consider in this work as mesons  $, , , , !$ , and  $.$

In order to distinguish the various sectors of  $H^{[2]}$ , we introduce corresponding projection operators  $P_N$ ,  $P$  and  $P_X$ , i.e., in symbolic notation

$$P_N H^{[2]} = H_{NN}^{[2]} ; \quad P H^{[2]} = H_N^{[2]} ; \quad P_X H^{[2]} = H_{XNN}^{[2]} : \quad (3)$$

Later we also will need the projection operator on the combined subspace  $H_{NN}^{[2]} \quad H_N^{[2]}$  which is given by  $P = P_N + P$ . Moreover, in view of the different subspaces in (2), it is useful to decompose the projection operator  $P_X$  into a sum of six orthogonal projectors corresponding to the six mesons considered

$$P_X = \begin{matrix} X \\ \times 2f ; ; ; ; ! ; g \end{matrix} \quad P_X ; \quad (4)$$

which are defined by

$$P_X H^{[2]} = H_{XNN}^{[2]} ; \quad \times 2f ; ; ; ; ! ; g : \quad (5)$$

Using the notation

$$= P \quad P ; \quad ; \quad 2 \text{ fN} ; \quad ; X g ; \quad (6)$$

any operator acting in  $H^{[2]}$  can be written as a symbolic 3 × 3 matrix

$$= \begin{matrix} 0 & & 1 \\ \emptyset & \begin{matrix} N & N \\ N & \end{matrix} & \begin{matrix} N & \\ N & X \\ X & \end{matrix} \\ \begin{matrix} X & N \\ X & \end{matrix} & \begin{matrix} X & \\ X & X \\ X & X \end{matrix} & A \end{matrix} : \quad (7)$$

### B. The Hamiltonian

The Hamiltonian operator  $H$  of our model can be divided into a kinetic part  $H_0$  and an interaction  $H_I$

$$H = H_0 + H_I ; \quad (8)$$

where the bar indicates that it refers to bare baryons. With respect to the matrix notation of (7),  $H_0$  is a diagonal one-body operator. Its nonvanishing elements are defined by

$$H_{0;NN} = h_N (1) + h_N (2) ; \quad (9)$$

$$H_{0;N} = h_N^{nr} + h ; \quad (10)$$

$$H_{0;XX} = h_N (1) + h_N (2) + h_X ; \quad (11)$$

with the kinetic energies of the bare and physical nucleons, respectively,

$$h_N (p^0) j_N (p) i = e_N (p) (p^0 - p) ; \quad (12)$$

$$h_N (p^0) j_N^{nr} (p) i = e_N^{nr} (p) (p^0 - p) ; \quad (13)$$

the nonrelativistic limit of the latter

$$h_N (p^0) j_N^{nr} (p) i = e_N^{nr} (p) (p^0 - p) ; \quad (14)$$

the kinetic energy of the bare resonance

$$h (p^0) j_N (p) i = e (p) (p^0 - p) ; \quad (15)$$

and of the mesons

$$h_X (q^0) j_X (q) i = (2 \pi)^3 2 !_X (q) (q^0 - q) \quad \text{for } X = f, \pi, \rho, \omega ; \quad (16)$$

In these equations, the kinetic energies of the mesons, bare and bare and physical nucleons (with masses  $m_X$ ,  $m_f$ ,  $m_\pi$ ,  $m_\rho$ ,  $m_\omega$ ,  $m_N$ , and  $M_N$ , respectively) are given by

$$!_X (p) = \frac{p}{m_X^2 + p^2} ; \quad (17)$$

$$e (p) = M^0 + \frac{p^2}{2M^0} ; \quad (18)$$

$$e_N (p) = \frac{q}{M_N^2 + p^2} ; \quad (19)$$

$$e_N (p) = \frac{q}{M_N^2 + p^2} ; \quad (20)$$

$$e_N^{nr} (p) = M_N + \frac{p^2}{2M_N} ; \quad (21)$$

where  $p = j p j$ . A few remarks concerning the relations in (10) and (11) are in order. Due to the truncation of the Hilbert space, no explicit dressing of the bare nucleon in  $H_N^{[2]}$  is possible. Therefore, we will use the physical instead of the bare nucleon mass in  $H_0$ , and  $H_{0;XX}$ , so that the formally suppressed meson-nucleon loops

in  $H_N^{[2]}$   $H_{XNN}^{[2]}$  can be taken into account at least effectively by the physical nucleon mass. For simplicity, we use in  $H_0$ , the nonrelativistic expressions for the kinetic energies of nucleon and isobar because we will treat the nonrelativistically. This approximation is, however, not crucial.

We now turn to the hadronic interaction  $H_I$ . In this context, it is useful to introduce new quantities  $H_0$  and  $V^0$  via

$$H = H_0 + V^0; \quad (22)$$

where the kinetic part  $H_0$  by definition refers to physical nucleons only, i.e.

$$H_{0;NN} = h_N (1) + h_N (2); \quad (23)$$

$$H_{0;N} = H_0; \quad ; \quad (24)$$

$$H_{0;XX} = H_{0;XX}; \quad ; \quad (25)$$

whereas

$$V^0 = H_I + H_0 - H_0 \quad (26)$$

contains besides the interaction  $H_I$ , which connects the various sectors of the Hilbert space, a so-called diagonal counter term

$$V^{[c]} = H_0 - H_0; \quad (27)$$

which is nonzero in  $H_{NN}^{[2]}$  only. Moreover it is a pure one-body operator

$$V_{NN}^{[c]} = \sum_{i=1,2}^X v_{NN}^{[c]} (i); \quad (28)$$

with

$$v_{NN}^{[c]} = h_N - h_N : \quad (29)$$

In the following, we will focus our attention on the components of  $V^0 = H_I + V^{[c]}$ , which are depicted in Fig. 1. For the purpose of this section, it is not necessary to specify them explicitly. It is sufficient to give a physical interpretation of them. We only need to know that the interaction will be such that the nondiagonal components  $V_{NX}^0$ ,  $V_{XN}^0$ ,  $V_{XN}^0$  and  $V_X^0$  are given as sums of one-body vertices

$$V_{XN}^0 = \sum_{i=1,2}^X v_{XN}^0 (i); \quad V_{NX}^0 = \sum_{i=1,2}^X v_{NX}^0 (i); \quad (30)$$

$$V_X^0 = \sum_{i=1,2}^X v_X^0 (i); \quad V_X^0 = \sum_{i=1,2}^X v_X^0 (i); \quad (31)$$

which describe the emission or absorption of a meson by one "active" baryon to which the argument "i" in (30) and (31) refers.

Besides the counter term  $V^{[c]}$  of (28), we allow in addition in  $V_{PP}^0$  a two-body part  $V_{PP}^{0[2]}$  which describes an *ab initio* given mean interaction between two baryons, i.e.,

$$V_{PP}^0 = V_{PP}^{[c]} + V_{PP}^{0[2]}; \quad (32)$$

which will be specified later. In the one-meson approximation, the remaining interaction  $V_{XX}^0$  consists in principle of two parts

$$V_{XX}^0 = V_{XX}^{0N} + \sum_{x2f; ; ; ; !; g}^X V_{XX}^{0x} : \quad (33)$$

The first one describes a meson-nucleon interaction with the other nucleon  $N$  as spectator and the second one two interacting nucleons with a meson  $x$  as spectator (see Fig. 1). In consequence,  $V_{XX}^{0N}$  can be written as a sum of one-nucleon terms

$$V_{X X}^{0 N} = \begin{matrix} X \\ v_{X X}^0 (i) : \\ i=1,2 \end{matrix} \quad (34)$$

In the previous work of Wilhelm et al. [3,22,23] and Bulla et al. [20],  $V_{X X}^0$  was neglected completely for practical reasons. Above the  $d$  threshold, however, this approximation leads to several problems, in particular with three-body unitarity (see the discussion in Sect. III D), which are solely due to the neglect of  $V_{X X}^0$ . We therefore set

$$V_{X X}^{0 N} = 0; \quad (35)$$

and for  $x \notin$

$$V_{X X}^{0 X} = 0; \quad (36)$$

whereas only  $V_{X X}^0$  will be retained nonzero.

### C. The physical nucleon

The Hilbert space  $H^{[1]}$  of the one-nucleon sector has an analogous structure as  $H^{[2]}$

$$H^{[1]} = H_N^{[1]} \quad H_{X N}^{[1]} : \quad (37)$$

Note that  $a$  will not appear because of isospin conservation and the one-meson approximation. By introducing corresponding projection operators  $P_N^{[1]}$  and  $P_X^{[1]}$ , a matrix representation analogous to (7) can be used for any operator acting in  $H^{[1]}$ . We now turn to the concept of a "physical" nucleon state  $|N i$ . By definition,  $|N i$  is the eigenstate of the Schrödinger equation

$$h|N(p)i = e_N(p)|N(p)i; \quad (38)$$

where the energy  $e_N(p)$  contains the physical nucleon mass and where the hamiltonian  $h$  in  $H^{[1]}$  has the following structure

$$h = h_0 + v^0 \quad (39)$$

with

$$h_{0;N N} = h_N; \quad (40)$$

$$h_{0;X X} = h_N + h_X; \quad (41)$$

and

$$v^0 = \begin{matrix} v_{N N}^0 & v_{N X}^0 \\ v_{X N}^0 & v_{X X}^0 \end{matrix} : \quad (42)$$

Since we do not consider a diagonal meson-nucleon interaction in  $H_{X N}^{[1]}$  (see (34) and (35)),  $v_{X X}^0$  is equal to zero. The matrix element  $v_{N N}^0$  is identical to the one-body counter term  $v^{[c]} = h_N - h_N$  in (28).

For the forthcoming discussion, it is useful to introduce the decomposition

$$|N i = P_N^{[1]}|N i + P_X^{[1]}|N i \quad (43)$$

of the physical nucleon into "nucleonic" and "mesonic" components. By definition,  $P_N^{[1]}|N i$  is proportional to the bare nucleon

$$P_N^{[1]}|N(p)i = N_{[1]}^{-1}(p)|N(p)i; \quad (44)$$

where  $N_{[1]}(p)$  is a renormalization constant to be discussed below. Using (43), it is straightforward to decompose equation (38) into two equations for  $P_N^{[1]}|N i$  and  $P_X^{[1]}|N i$  via

$$h_0 + v_{NN}^{[c]} + v_{NN}^0 g_0(e_N(p)) v_{NN}^0 P_N^{[1]} \mathcal{N}(p)i = e_N(p) P_N^{[1]} \mathcal{N}(p)i; \quad (45)$$

$$g_0(e_N(p)) v_{NN}^0 P_N^{[1]} \mathcal{N}(p)i = P_N^{[1]} \mathcal{N}(p)i; \quad (46)$$

where the free propagator  $g_0(z)$  is defined by

$$g_0(z) = (z - h_0)^{-1}; \quad (47)$$

In consequence, the physical nucleon state can be written as

$$\mathcal{N}(p)i = N_{[1]}^{-1}(p) 1 + g_0(e_N(p)) v_{NN}^0 \mathcal{N}(p)i \quad (48)$$

with the renormalization constant

$$N_{[1]}(p) = \frac{q}{1 + v_{[1]}^2(p)}; \quad (49)$$

where  $v_{[1]}^2(p)$  is defined by

$$hN(p^0) j_{NN}^0 g_0(e_N(p^0)) g_0(e_N(p)) v_{NN}^0 \mathcal{N}(p)i = v_{[1]}^2(p) (p^0 - p); \quad (50)$$

These considerations allow us also to determine the counter term  $v_{NN}^{[c]}$ . With the help of

$$e_N(p) P_N^{[1]} \mathcal{N}(p)i = h_0 P_N^{[1]} \mathcal{N}(p)i; \quad (51)$$

equation (45) yields the identity

$$hN(p^0) j_{NN}^{[c]} \mathcal{N}(p)i = hN(p) j_{NN}^0 (e_N(p) - h_0) v_{NN}^0 \mathcal{N}(p)i (p^0 - p); \quad (52)$$

so that  $v_{NN}^{[c]}$  compensates the term  $v_{NN}^0 g_0(e_N(p)) v_{NN}^0$  on the left hand side of (45).

For the following discussions it is useful to introduce the following compact expression for  $v_{NN}^{[c]}$

$$v_{NN}^{[c]} = \frac{1}{dz} (z - H_0) v_{NN}^0 g_0(z) v_{NN}^0; \quad (53)$$

In summary, it is obvious that a distinction between bare and physical nucleons is necessary due to the occurrence of the interaction  $v_{NN}^0$ . Otherwise, intermediate meson-nucleon loops, generated by the term  $v_{NN}^0 g_0(e_N(p)) v_{NN}^0$  in (45), would be counted twice in the physical nucleon state  $\mathcal{N}i$ .

### D. NN scattering

Now we will come back to the two-nucleon sector for the study of NN scattering. The scattering states  $\mathcal{N}N; p; i^{(1)}$  in the cm. system with the asymptotic free relative momentum  $p$ , energy  $E_p^{NN} = 2e_N(p)$  and a complete set of internal quantum numbers are given by

$$\mathcal{N}N; p; i^{(1)} = N_{[2]}^{-1}(p) 1 + G_0(E_p^{NN} - i) T^0(E_p^{NN} - i) \mathcal{N}N; p; i; \quad (54)$$

where  $N_{[2]}(p)$  is a renormalization constant which appears because both, the free bare as well as the physical two-nucleon states are normalized to the  $i$  function. The transition amplitude  $T^0$  satisfies the Lippmann-Schwinger equation

$$T^0(z) = V^0 + V^0 G_0(z) T^0(z) \quad (55)$$

with the free propagator  $G_0$

$$G_0(z) = (z - H_0)^{-1}; \quad (56)$$

which is represented in Fig. 2.

With the help of projection operators one can bring (54) into the equivalent form

$$\begin{aligned} \mathcal{N}N; p; i^{(1)} &= N_{[2]}^{-1}(p) 1 + G_0(E_p^{NN} - i) T_{PN}^0(E_p^{NN} - i) \\ &+ G_0(E_p^{NN} - i) T_{XN}^0(E_p^{NN} - i) \mathcal{N}N; p; i; \end{aligned} \quad (57)$$

where  $T_{PP}^0$  and  $T_{XP}^0$  are given by (note  $P = P_N + P_X$ )

$$T_{PP}^0(z) = V_{PP}^0(z) + V_{PP}^0(z)G_0(z)T_{PP}^0(z); \quad (58)$$

$$T_{XP}^0(z) = G_0^{-1}(z)G^X(z)V_{XP}^0 1 + G_0(z)T_{PP}^0(z); \quad (59)$$

In these relations,  $V_{PP}^0$  and  $G^X$  are defined by

$$V_{PP}^0(z) = V_{PP}^0 + V_{PX}^0 G^X(z)V_{XP}^0; \quad (60)$$

and

$$\begin{aligned} G^X(z) &= (z - H_{0,XX} - V_{XX}^0)^{-1} \\ &= G_0(z) + G_0(z)T^X(z)G_0(z); \end{aligned} \quad (61)$$

where we have introduced for later purpose the  $NN$  scattering matrix  $T^X(z)$  in the presence of a spectator meson which fulfills the equation

$$T^X(z) = V_{XX}^0 + V_{XX}^0 G_0(z)T^X(z); \quad (62)$$

Its diagrammatic representation is shown in Fig. 3.

The driving term  $V_{PP}^0$  in (60) can now be split into a connected ("con") and a disconnected ("dis") part

$$V_{PP}^0(z) = V_{PP}^{0;dis}(z) + V_{PP}^{0;con}(z); \quad (63)$$

where by definition,  $V_{PP}^{0;dis}$  contains only those parts of the driving term  $V_{PP}^0$  which do not describe an interaction between the two nucleons, whereas  $V_{PP}^{0;con}(z)$  contains besides  $NN$  loop contributions to the selfenergy the genuine baryon-baryon interaction. In detail one finds from (60) and (61) with (32)

$$V_{PP}^{0;dis}(z) = V_{NN}^{[c]} + V_{NX}^0 G_0(z)V_{XN}^0 \text{dis}; \quad (64)$$

$$\begin{aligned} V_{PP}^{0;con}(z) &= V_{PP}^{0[2]} + V_{PX}^0 G_0(z)V_{XP}^0 \text{con} + V_{PX}^0 G_0(z)T^X(z)G_0(z)V_{XP}^0 \\ &+ V_X^0 G_0(z)V_X^0 \text{dis}; \end{aligned} \quad (65)$$

where we have defined

$$V_X^0 G_0(z)V_X^0 \text{dis} = \sum_{i=1,2}^X v_X^0(i)G_0(z)v_X^0(i); \quad 2 \text{ fN; g}; \quad (66)$$

$$V_X^0 G_0(z)V_X^0 \text{con} = \sum_{i,j=1,2; j \neq i}^X v_X^0(i)G_0(z)v_X^0(j); \quad ; \quad 2 \text{ fN; g}; \quad (67)$$

Thus the connected part  $V_{PP}^{0;con}(z)$ , which is shown in Fig. 4, contains besides  $V_{PP}^0$  a retarded one-boson exchange interaction, the coupling to the  $NN$  channel, and, furthermore, also a disconnected part, namely, the already mentioned  $NN$  loop contributions to the selfenergy in the last term of (65). The separation (63) allows us to apply the two-potential formula to (58) (see the appendix) and to represent the total amplitude by a "disconnected"  $T_{PP}^{0;dis}(z)$  and a "connected"  $T^{0;con}(z)$  amplitude

$$T_{PP}^0(z) = T_{PP}^{0;dis}(z) + 1 + T_{PP}^{0;dis}(z)G_0(z) T_{PP}^{0;con}(z) 1 + G_0(z)T_{PP}^{0;dis}(z); \quad (68)$$

where

$$T_{PP}^{0;dis}(z) = V_{PP}^{0;dis}(z) + V_{PP}^{0;dis}(z)G_0(z)T_{PP}^{0;dis}(z); \quad (69)$$

$$T_{PP}^{0;con}(z) = V_{PP}^{0;con}(z) + V_{PP}^{0;con}(z)G_0(z)T_{PP}^{0;con}(z); \quad (70)$$

with the dressed propagator

$$\begin{aligned}\mathcal{G}_0(z) &= (z - H_0 - V_{PP}^{0;dis}(z))^{-1} \\ &= G_0(z) + G_0(z)T_{PP}^{0;dis}(z)G_0(z) : \end{aligned}\quad (71)$$

A graphical representation of the dressed propagator in the form  $\mathcal{G}_0(z) = G_0(z) + G_0(z)V_{PP}^{0;dis}(z)\mathcal{G}_0(z)$  is displayed in Fig. 5 and of the connected scattering amplitude  $T_{PP}^{0;con}(z)$  in Fig. 6.

We are now in the position to rewrite the relation (54) for the NN scattering states with the help of Eqs. (57)–(59), (68) and (71) as follows

$$\begin{aligned}\mathcal{N}N; p; i^{(1)} &= N_{[2]}^{-1}(p) 1 + G^X(E_p^{NN} - i)V_{XP}^0 1 + \mathcal{G}_0(E_p^{NN} - i)T_{PP}^{0;con}(E_p^{NN} - i) \\ &\quad 1 + G_0(E_p^{NN} - i)T_{PP}^{0;dis}(E_p^{NN} - i) \mathcal{N}N; p; i : \end{aligned}\quad (72)$$

This relation is of central importance to this work and thus we will discuss its properties in greater detail. At first, let us consider the special case of two noninteracting physical nucleons denoted by  $\mathcal{N}N; p; i$ . This state can be obtained from Eq. (72) by neglecting all connected interaction terms, i.e., by setting  $T_{PP}^{0;con} = 0$  and replacing  $G^X$  by  $G_0$ . Using the decomposition

$$\mathcal{N}N; p; i = P_N \mathcal{N}N; p; i + P_X \mathcal{N}N; p; i \quad (73)$$

into nucleonic and mesonic components, one obtains for example for  $P_N \mathcal{N}N; p; i$  the Lippmann–Schwinger equation

$$P_N \mathcal{N}N; p; i = N_{[2]}^{-1}(p) 1 + G_0(E_p^{NN} - i)T_{PP}^{0;dis}(E_p^{NN} - i) \mathcal{N}N; p; i : \quad (74)$$

which is equivalent to the Schrödinger equation

$$H_0 + V_{PP}^{0;dis}(E_p^{NN}) P_N \mathcal{N}N; p; i = E_p^{NN} \mathcal{N}N; p; i : \quad (75)$$

This relation allows us to determine the counterterm  $V_{NN}^{[c]}$  in the two-nucleon sector. In view of  $P_N \mathcal{N}N; p; i = \mathcal{N}N; p; i$  and the trivial identity  $H_0 P_N \mathcal{N}N; p; i = E_p^{NN} \mathcal{N}N; p; i$ , one finds for the counterterm (note the analogy to the one-nucleon sector)

$$V_{NN}^{[c]} = \int^z dz (z - H_0) V_{NX}^0 G_0(z) V_{XN}^0 : \quad (76)$$

It should be emphasized that due to the one-meson approximation, one has to face the pathological situation that a dressing of both nucleons at the same time is not possible. Therefore,  $\mathcal{N}N; p; i$  is not the direct product of two physical nucleon states of the one-nucleon sector, i.e.,

$$\mathcal{N}N; p; i \neq \mathcal{N}(p)i \mathcal{N}(p)i : \quad (77)$$

A way out of this well known problem [24] could be the so-called "convolution approach" of Blankleider and Kvinikhidze [25,27], which for technical reasons has not yet been implemented in our model.

In order to account for the nucleon dressing, we will introduce the two-body renormalization operator  $\mathcal{B}_{[2]}$  defined as

$$\mathcal{B}_{[2]}^2(z) = 1 + \int^z dz^0 (z^0 - H_0) V_{NX}^0 G_0(z^0) G_0(z) V_{XN}^0 : \quad (78)$$

which differs from unity in  $H_{NN}^{[2]}$  only. For later purpose we introduce furthermore its onshell value by

$$(\mathcal{B}_{[2]}^{\text{os}})^2 = 1 + \int^z dz^0 (z^0 - H_0) V_{NX}^0 G_0(z^0) G_0(z^0) V_{XN}^0 : \quad (79)$$

With the help of  $\mathcal{B}_{[2]}(z)$ , one can rewrite the dressed propagator  $\mathcal{G}_0(z)$  according to

$$\mathcal{G}_0(z) = G_0(z) \mathcal{B}_{[2]}^2(z) : \quad (80)$$

and one obtains from (71) the identity

$$1 + G_0(z) T_{p,p}^{0;\text{dis}}(z) = \mathcal{D}_{[2]}^2(z); \quad (81)$$

which allows us to determine the unknown renormalization constant  $N_{[2]}(p)$  straightforwardly. From the normalization condition

$$h_{NN; p^0; 0} \mathcal{J}_{NN; p; i} = 0 \quad (\mathbf{p}^0 = \mathbf{p}); \quad (82)$$

one finds

$$h_{NN; p^0; j} \mathcal{D}_{[2]}^{j;\text{dis}}(z) = N_{[2]}(p) \quad (\mathbf{p}^0 = \mathbf{p}); \quad (83)$$

Another useful quantity is the so-called "dressing operator" which is defined by

$$\mathcal{R}(z) = \mathcal{D}_{[2]}^{0;\text{dis}} \mathcal{D}_{[2]}^{-1}(z); \quad (84)$$

Thus  $\mathcal{R}(z)$  is equal to the identity for onshell particles.

Introducing in addition "renormalized" interactions via

$$V = (\mathcal{D}_{[2]}^{0;\text{dis}})^{-1} V^0 (\mathcal{D}_{[2]}^{0;\text{dis}})^{-1}; \quad \text{for } V^0 = 2 f_P X g; \quad (85)$$

$$V_{p,p}^{\text{con}}(z) = (\mathcal{D}_{[2]}^{0;\text{dis}})^{-1} V_{p,p}^{0;\text{con}}(z) (\mathcal{D}_{[2]}^{0;\text{dis}})^{-1}; \quad (86)$$

one obtains for the renormalized amplitude

$$\begin{aligned} T_{p,p}^{\text{con}}(z) &= \mathcal{R}(z) (\mathcal{D}_{[2]}^{0;\text{dis}})^{-1} T_{p,p}^{0;\text{con}}(z) (\mathcal{D}_{[2]}^{0;\text{dis}})^{-1} \mathcal{R}(z) \\ &= \mathcal{D}_{[2]}^{-1}(z) T_{p,p}^{0;\text{con}}(z) \mathcal{D}_{[2]}^{-1}(z) \end{aligned} \quad (87)$$

from Eq. (70) the Lippmann-Schwinger equation

$$T_{p,p}^{\text{con}}(z) = \mathcal{R}(z) V_{p,p}^{\text{con}}(z) \mathcal{R}(z) + \mathcal{R}(z) V_{p,p}^{\text{con}}(z) \mathcal{R}(z) G_0(z) T_{p,p}^{\text{con}}(z); \quad (88)$$

The renormalized amplitude  $T_{p,p}^{\text{con}}(z)$  is very useful for practical evaluations. For example, let us consider  $NN$  scattering for which the  $T$ -matrix element is given by the onshell matrix element of  $T^0$

$$N_{[2]}^2(p) h_{NN; p^0; 0} \mathcal{J}^0(E_p^{NN} + i) \mathcal{J}_{NN; p; i}; \quad (89)$$

where  $\mathbf{p}^0 j = \mathbf{p} j = \mathbf{p}$  has been used. With the help of (81), the total amplitude  $T_{p,p}^0$  (Eq. (68)) can be rewritten according to

$$T_{p,p}^0(z) = T_{p,p}^{0;\text{dis}}(z) + \mathcal{D}_{[2]}^{-1}(z) T_{p,p}^{\text{con}}(z) \mathcal{D}_{[2]}^{-1}(z); \quad (90)$$

Remembering Eq. (83) and with the relation

$$\begin{aligned} T_{p,p}^{\text{dis}}(z) \mathcal{J}_{NN; p; i} &= G_0^{-1}(z) \mathcal{D}_{0; p,p}(z) - 1 G_0^{-1}(z) \mathcal{J}_{NN; p; i} \\ &= \mathcal{D}_{[2]}^2(z) - 1 G_0^{-1}(z) \mathcal{J}_{NN; p; i}; \end{aligned} \quad (91)$$

which vanishes for  $z = E_p^{NN} - i$ , one finds for the matrix element in Eq. (89)

$$\begin{aligned} N_{[2]}^2(p) h_{NN; p^0; 0} \mathcal{J}^0(E_p^{NN} + i) \mathcal{J}_{NN; p; i} &= \\ h_{NN; p^0; 0} \mathcal{J}_{NN; p; i}^{\text{con}}(E_p^{NN} + i) \mathcal{J}_{NN; p; i} & \end{aligned} \quad (92)$$

Thus  $NN$  scattering is unambiguously fixed by the onshell matrix element of  $T_{p,p}^{\text{con}}$ . However, for our future application to electromagnetic deuteron break-up, we need the half-off-shell continuation of  $T_{p,p}^{\text{con}}$ , in addition with the baryonic and mesonic components of the  $NN$  scattering states. Explicitly, one obtains in conjunction with (72) and (80) through (87) the following expressions ( $z = E_p^{NN} - i$ )

$$P_N \bar{N}N; p; i^{(1)} = \frac{\bar{P}(z)}{\bar{D}_{[2]}^{os}} (1 + G_0(z) T_{PP}^{con}(z)) \bar{N}N; p; i; \quad (93)$$

$$P_X \bar{N}N; p; i^{(1)} = G^X(z) V_{XN} \bar{P}(z) (1 + G_0(z) T_{PP}^{con}(z)) \bar{N}N; p; i; \quad (94)$$

At the end of this subsection we would like to discuss briefly the incorporation of the  $N$  loop contributions to the selfenergy, which are still contained in  $V^{con}(z)$ , by introducing a two-baryon propagator with a dressed  $\bar{P}$ . To this end, we subdivide the driving term  $V_{PP}^{con}(z)$  of (88) into two parts

$$V_{PP}^{con}(z) = V_{[1]PP}^{con}(z) + V_{[2]PP}^{con}(z); \quad (95)$$

where

$$V_{[1]PP}^{con}(z) = V_X^0 G_0(z) V_{XN}^0 \text{dis}; \quad (96)$$

$$V_{[2]PP}^{con}(z) = V_{PP}^0 + V_{PX}^0 G_0(z) V_{XP}^0 \text{con} + V_{PX}^0 G_0(z) T^X(z) G_0(z) V_{XP}^0; \quad (97)$$

The term  $V_{[1]PP}^{con}(z)$  contains solely the intermediate  $N$  loops. Due to the separable structure of  $V_{[1]PP}^{con}(z)$ , the application of the two-potential formula is particularly useful and leads to the following expression for  $T_{PP}^{con}(z)$

$$T_{PP}^{con}(z) = G_0^{-1}(z) G_0^{(1)}(z) + G_0^{(1)}(z) \bar{P}_{PP}^{con}(z) G_0^{(1)}(z) G_0^{-1}(z) G_0^{-1}(z); \quad (98)$$

The auxiliary amplitude  $\bar{P}_{PP}^{con}(z)$  is given by the integralequation

$$\bar{P}_{PP}^{con}(z) = V_{[2]PP}^{con}(z) + V_{[2]PP}^{con}(z) G_0^{(1)}(z) \bar{P}_{PP}^{con}(z); \quad (99)$$

where we have introduced another "dressed" propagator

$$G_0^{(1)}(z) = G_0(z) + G_0(z) V_{[1]PP}^{con}(z) G_0^{(1)}(z); \quad (100)$$

which takes into account the dressing of the  $\bar{N}$  in  $H_N^{[2]}$ . In  $H_{NN}^{[2]}$  and  $H_{XNN}^{[2]}$ ,  $G_0^{(1)}(z)$  is identical to the free propagator, i.e.

$$G_{0;NN}^{(1)}(z) = G_{0;NN}(z); \quad G_{0;XX}^{(1)}(z) = G_{0;XX}(z); \quad (101)$$

whereas in  $H_N^{[2]}$  one gets a simple connection between  $G_0^{(1)}(z)$  and the propagator  $g(z)$  in the one- sector (see Sect. III B) according to

$$h_N; p^0 G_0^{(1)}(z) \bar{N}; p i = h; p^0 g(z) - M_N - \frac{p^2}{2_N} j; p i; \quad (102)$$

where  $p$  is the relative momentum of the  $N$  system, and its reduced mass is denoted by

$$M_N = \frac{M^0 M_N}{M^0 + M_N}; \quad (103)$$

With (98), we obtain from (93) and (94) the following explicit expressions for the baryonic and mesonic components of the  $NN$  scattering states ( $z = E_p^{NN}$ ,  $i$ )

$$P_N \bar{N}N; p; i^{(1)} = \frac{\bar{P}(z)}{\bar{D}_{[2]}^{os}} (1 + G_0(z) \bar{P}_{NN}^{con}(z)) \bar{N}N; p; i; \quad (104)$$

$$P_X \bar{N}N; p; i^{(1)} = G_0^{(1)}(z) \bar{P}_{NN}^{con}(z) \bar{N}N; p; i; \quad (105)$$

$$P_X \bar{N}N; p; i^{(1)} = G^X(z) V_{XN} \bar{P}(z) (1 + G_0(z) \bar{P}_{NN}^{con}(z)) \bar{N}N; p; i + G^X(z) V_{XN} G_0^{(1)}(z) \bar{P}_{NN}^{con}(z) \bar{N}N; p; i; \quad (106)$$

Due to its vanishing isospin, the deuteron cannot contain a  $N^-$  component. Thus, the deuteron state  $\mathbf{j}_{\text{di}}$  can be separated (similar to the free state of two noninteracting physical nucleons (consider (73)) into a nucleonic and a mesonic component

$$\mathbf{j}_{\text{di}} = P_N \mathbf{j}_{\text{di}} + P_X \mathbf{j}_{\text{di}}; \quad (107)$$

which can be determined by the Schrödinger equation in the cm. frame

$$H_0 + V^0 \mathbf{j}_{\text{di}} = M_d \mathbf{j}_{\text{di}} \quad (108)$$

with  $M_d = 2M_N - B$  as deuteron mass and  $B$  its binding energy. Eq. (108) is equivalent to

$$H_{0;NN} + V_{NN}^{[c]} + V_{NN}^{0[2]} + V_{NX}^0 \frac{P_N \mathbf{j}_{\text{di}}}{P_X \mathbf{j}_{\text{di}}} = M_d \frac{P_N \mathbf{j}_{\text{di}}}{P_X \mathbf{j}_{\text{di}}} : \quad (109)$$

Note that in our realization we have set  $V_{NN}^0 = 0$  for the isospin  $t=0$  channels as will be discussed in Sect. III D. Elimination of the "mesonic" component  $P_X \mathbf{j}_{\text{di}}$  by

$$P_X \mathbf{j}_{\text{di}} = G_0 (M_d) V_{XN}^0 \mathbf{j}_{\text{di}}; \quad (110)$$

yields for the "nucleonic" component the equation

$$H_0 + V_{NN}^{[c]} + V_{NN}^{0[2]} + V_{NX}^0 G_0 (M_d) V_{XN}^0 P_N \mathbf{j}_{\text{di}} = M_d P_N \mathbf{j}_{\text{di}}; \quad (111)$$

Using the renormalization operator  $\hat{Z}_{[2]}$  given in (78), it is straightforward to rewrite the operator on the left hand side of (111) according to

$$\begin{aligned} H_0 + V_{NN}^{[c]} + V_{NN}^{0[2]} + V_{NX}^0 G_0 (M_d) V_{XN}^0 \\ = H_0 + V_{NN}^{[c]} + V_{NN}^{0[2]} + V_{NX}^0 G_0 (M_d) V_{XN}^0_{\text{dis}} + V_{NX}^0 G_0 (M_d) V_{XN}^0_{\text{con}} \\ = H_0 + V_{NN}^{0[2]} + (M_d - H_0) (1 - \hat{Z}_{[2]}^2 (M_d)) + V_{NX}^0 G_0 (M_d) V_{XN}^0_{\text{con}} : \end{aligned} \quad (112)$$

Consequently, one obtains an equation for the "nucleonic" component

$$G_0 (M_d) \hat{Z}_{[2]}^2 (M_d) + V_{NN}^{0[2]} + V_{NX}^0 G_0 (M_d) V_{XN}^0_{\text{con}} P_N \mathbf{j}_{\text{di}} = 0 : \quad (113)$$

We now introduce in  $H_{NN}^{[2]}$  this component as an effective renormalized deuteron state by

$$\mathbf{j}_{\text{di}} = \hat{Z}_{[2]} (M_d) P_N \mathbf{j}_{\text{di}}; \quad (114)$$

with the normalization  $\hbar \mathbf{j}_{\text{di}} = 1$ . In conjunction with (85) and (86) one finds for  $\mathbf{j}_{\text{di}}$  the equation

$$H_0 + \hat{R} (M_d) V_{NN}^{[2]} (M_d) + V_{NX}^0 G_0 (M_d) V_{XN}^0 \mathbf{j}_{\text{con}} \hat{R} (M_d) \mathbf{j}_{\text{di}} = M_d \mathbf{j}_{\text{di}}; \quad (115)$$

which contains only renormalized quantities. Here,  $V_{NN}^{[2]}$  is obtained from  $V_{NN}^{0[2]}$  by renormalization analogous to (85). Note that the effective potential is the driving term of  $T_{PP}^{\text{con}}(z)$  for the isospin  $t=0$  channels (cf. (65) and (88)).

Summarizing, the deuteron state  $\mathbf{j}_{\text{di}}$  is given by

$$\mathbf{j}_{\text{di}} = \frac{1}{N_d} \frac{\hat{R} (M_d)}{\hat{Z}_{[2]}^{\text{pos}}} + G_0 (M_d) V_{XN}^0 \hat{R} (M_d) \mathbf{j}_{\text{di}} : \quad (116)$$

From the condition  $\hbar \mathbf{j}_{\text{di}} = 1$  one obtains for the renormalization constant  $N_d$

$$N_d^2 = \hbar \mathbf{j}_{\text{di}} \cdot \frac{1}{\hat{Z}_{[2]}^{\text{pos}}} \int_{z=M_d}^{\infty} \hat{R} (z) V_{XN}^0 G_0 (z) V_{XN}^0 \mathbf{j}_{\text{con}} \hat{R} (z) \mathbf{j}_{\text{di}} : \quad (117)$$

Due to the absence of  $N$  components and the vanishing of  $V_{NN}^0$  in ( $t = 0$ ) channels, the quantity  $V_{NN}^{[2]}$  in (115) can be put equal to zero in retarded calculations (see the discussion in the next section and in particular (169)). In static approaches, the situation becomes even simpler. Because of the choice  $V_{NN}^0 = 0$ , Eqs. (110) and (111) simplify to

$$H_0 + V_{NN}^{[2]} P_N \not{p}_i = M_d P_N \not{p}_i; \quad (118)$$

$$P_X \not{p}_i = 0; \quad (119)$$

In this case,  $V_{NN}^{[2]}$  has to be identified with the chosen realistic  $NN$  potential  $V_{NN}^{\text{real}}$  (see the next section).

### III. FIELD-THEORETICAL REALIZATION

Until now, the hadronic interaction has not been specified in detail in order to keep the discussion as general as possible. Now, we will introduce a field-theoretical realization. In view of various approaches in the literature, it will be useful to distinguish two types of realizations which differ in the treatment of the interaction in  $H_{NN}^{[2]}$  only, i.e., in  $V_{NN}^{0;\text{con}}$  and which we will coin "static" and "retarded" approaches. In order to illustrate the essential differences, we will neglect for the moment being the isobar, and also  $V_{XX}^0$  is set equal to zero for simplicity. Then the pure nucleonic component of the driving term  $V_{PP}^{0;\text{con}}$ , defined in (65), of the scattering amplitude  $T_{PP}^{0;\text{con}}(z)$  in (70) simplifies to

$$V_{NN}^{0;\text{con}}(z) = V_{NN}^{[2]} + V_{NX}^0 G_0(z) V_{XN}^0 \text{con}; \quad (120)$$

It consists of two contributions:

- (i) a given mean field, energy independent potential  $V_{NN}^{[2]}$ , and
- (ii) a retarded one-meson exchange potential

$$V_{NN}^{0\text{ret}}(z) = V_{NX}^0 G_0(z) V_{XN}^0 \text{con}; \quad (121)$$

Now, the completely static approach is defined by the vanishing of any explicit meson-nucleon vertex, i.e.,  $V_{NX}^0 = 0$ , whereas for the completely retarded approach one chooses  $V_{NX}^0 \neq 0$  and  $V_{NN}^{[2]} = 0$ .

In the first case, the retarded one-meson exchange  $V_{NN}^{0\text{ret}}$  vanishes identically and the  $NN$  interaction  $V_{NN}^{0;\text{con}}$  is generated by  $V_{NN}^{[2]}$  alone. Furthermore, there would be no distinction between a bare and a physical nucleon according to (48), and the operators  $\mathcal{D}_{[2]}$  and  $\mathcal{R}$  are both equal to the identity. Consequently, one could then leave out the "bar" in the notation. In order to have a realistic description, one then has to identify  $V_{NN}^{[2]}$  with a realistic  $NN$  potential model  $V_{NN}^{\text{real}}$ , i.e.,

$$V_{NN}^{0;\text{con}}(z) = V_{NN}^{[2]} = V_{NN}^{\text{real}}; \quad (122)$$

One should note, however, that even in the static approach retardation is still contained in the interaction  $V^{0;\text{con}}$  (see diagram (c) of Fig. 8). Furthermore, one has to keep in mind that due to the coupling to the  $N$  and  $NN$  states, the realistic potential has to be renormalized in order to avoid double counting of parts of the interaction as will be discussed below in Sect. III E. Such an approach has been used in [18,19] and also in the coupled channel calculation of [13,23]. The obvious advantage of this framework is its simplicity. For excitation energies up to about 500 MeV, only pions could be created via the  $N$  vertex, whereas the heavier mesons are "frozen out".

In the retarded approach, on the other hand, neglecting  $V_{NN}^0$  and  $V_{XN}^0$ , the  $NN$  interaction is generated completely by the retarded one-meson exchange part  $V_{NN}^{0\text{ret}}(z)$ . In order to obtain a realistic description, one then has to consider besides the pion also heavier mesons explicitly. Otherwise, the  $NN$  interaction would be generated by a retarded one-pion exchange potential only, which would result in a rather crude description of experimental data. In the present work, we use the potential of Elster et al. [28,29], which will be discussed in some more detail in Sect. III F. Also in this case a renormalization of the  $NN$  potential will be needed if one includes explicitly the  $N$  and  $NN$  channels.

It is obvious that besides these two extremes various alternatives are possible. For example, Bulla and Sauer [20] used in their extension of the original model [18,19] the choice

$$V_N^0 \neq 0; \quad V_{NX}^0 = 0; \quad x 2 f; !; ; ; g; \quad V_{NN}^{[2]} = V_{NN}^{\text{real}} \quad V_{NN}^{0\text{ret}}(z = 2M_N); \quad (123)$$

and for  $V_{NN}^{\text{real}}$  the Paris potential [30], which has been renormalized with respect to  $N$  exchange in order to avoid double counting as will be discussed in detail below in Sect. III E.

### A. The component $V_{N_x}^0$

As discussed previously, the components  $V_{N_x}^0$  and  $V_{X_N}^0 = V_{N_x}^0 \gamma^5$  are explicitly present in retarded calculations only. For the  $m$  meson-nucleon vertices we have taken the usual couplings for pseudoscalar, scalar, and vector  $m$  mesons. Defining in general the  $xN$  vertex function for a  $m$  meson  $x$ , which enter (30), by

$$V_{N_x}^0(p^0, p; q) = h_N p^0 \gamma^0 \gamma_{N_x}^0 N(p; x) q_i; \quad (124)$$

one finds in detail the following expressions for the various  $m$  meson types:

(i) pseudoscalar mesons ( $x 2 f$ ;  $g$ ):

$$V_{N_x}^0(p^0, p; q) = g_x^0 u(p^0; 0) i^5 u(p; ) F_x(q^2) o : \quad (125)$$

(ii) scalar mesons ( $x 2 f$ ;  $g$ ):

$$V_{N_x}^0(p^0, p; q) = g_x^0 u(p^0; 0) u(p; ) F_x(q^2) o : \quad (126)$$

Like for the Bonn potentials [17,29], we will consider for exchange both, isovector and isoscalar exchange.

(iii) vector  $m$  mesons ( $x 2 f$ ;  $g$ ):

$$\begin{aligned} V_{N_x}^0(p^0, p; q) = & \gamma_x(q; s) u(p^0; 0) [g_x^0 + f_x^0] \\ & \frac{f_x^0}{2M_N} (p + p^0) u(p; ) F_x(q^2) o : \end{aligned} \quad (127)$$

In these expressions,  $u(p; )$  denotes the spinor of a bare nucleon with momentum  $p$  and spin projection  $, q$  the momentum of the  $m$  meson, and  $\gamma_x(q; s)$  the polarization vector of a vector  $m$  meson. For the isospin operator one has  $o = 1$  for isoscalar and  $o = -1$  for isovector exchange. The bare  $m$  meson-nucleon couplings are denoted by  $f_x^0$  and  $g_x^0$ . Furthermore, one should note that in principle, due to the one- $m$  meson approximation, the nucleons in the initial and final state would have different masses, i.e.,  $M_N$  or  $M_{N'}$  if the  $m$  meson is present or not, respectively. However, in order to avoid such a pathology, we always take the physical nucleon mass  $M_N$  in the above expressions.

Finally,  $F_x(q^2)$  denotes a phenomenological hadronic form factor, which has been associated with each vertex. It is parameterized in the conventional monopole ( $n_x = 1$ ) or dipole ( $n_x = 2$ ) form

$$F_x(q^2) = \frac{\frac{2}{x} \frac{m_x^2}{q^2}^{n_x}}{\frac{2}{x} + q^2} ; \quad x 2 f ; ; ; ; !; g; \quad (128)$$

where the cut-off parameters  $x$  are treated as free parameters to be fixed by fitting the  $NN$  scattering data below threshold and the deuteron properties.

### B. The coupling $V_x^0$

In  $H_N^{[2]}$ , the renormalization operator in (78) is the identity, so that no differentiation between bare and physical coupling has to be considered. In view of the strong coupling of the isobar to the  $N$  system, we restrict ourselves to  $V_x^0$  only, i.e.,

$$V_x^0 = 0; \quad \text{for } x 2 f ; !; ; ; g : \quad (129)$$

For the interaction  $V^0$  we take the usual nonrelativistic form for the one-body vertices of (31), defined in analogy to (124)

$$V^0(p^0, p; q) = i \frac{f_N^0}{m} \gamma^5; \quad \gamma^5 \sim_N \gamma_N; \quad F_N(q^2) \sim_N; \quad ; \quad (130)$$

where  $\gamma^5$  and  $\gamma_N$  denote the nonrelativistic and nucleon spinors, respectively, and the spin and isospin transition operators  $\sim_N$  and  $\sim_N$  are fixed by the reduced matrix elements

$$\frac{h_2^3}{2} \bar{J}^{\frac{11}{2}} \bar{J}^{\frac{11}{2}} i = \frac{h_2^3}{2} \bar{J}^{\frac{11}{2}} \bar{J}^{\frac{11}{2}} i = 2 : \quad (131)$$

Again a phenomenological form factor

$$F_N(q^2) = \frac{\frac{2}{N} m^2}{\frac{2}{N} + q^2} \quad (132)$$

has been introduced. Similar to [13,19], the free parameters  $f_N^0$  and  $m_N$  are fixed by fitting  $N$  scattering in the  $P_{33}$  channel. The amplitude  $t_N(z)$  for  $N$  scattering is obtained from

$$t_N(z) = v^0 + v^0 g_0(z) t_N(z); \quad (133)$$

where  $v^0$  contains all one-particle contributions of  $V^0$ , i.e.,

$$v^0 = \begin{pmatrix} 0 & v_{NN}^{[c]} & 0 & v_{N\chi}^0 & 1 \\ 0 & 0 & 0 & v_{N\chi}^0 & A \\ v_{\chi N}^0 & v^0 & 0 & 0 & \end{pmatrix} : \quad (134)$$

Restricting ourselves to the  $P_{33}$  channel, only the  $N$  interaction  $v^0$  has to be taken into account. The relevant projection  $t_N^{P_{33}}(z)$  for fixing the  $P_{33}$  scattering phase yields

$$t_N^{P_{33}}(z) = v^0 g(z) v^0; \quad (135)$$

where the dressed propagator  $g$ , depicted in Fig. 7, is given by

$$g(z) = (z - M^0 - \Sigma(z))^{-1} \quad (136)$$

with the selfenergy

$$\Sigma(z) = v^0 g_0(z) v^0 : \quad (137)$$

Because of our choice  $v_{\chi\chi}^0 = 0$  and the one-meson approximation, background mechanism like, e.g., the so-called Chew-Low term have to be neglected as in [13,19].

In the cm. frame, the  $P_{33}$  scattering phase  $\delta_{33}(W)$  is defined by

$$h_N; q \not\perp_N^{P_{33}}(W + i) \not\perp_N; q i = h_N; q \not\perp_N^{P_{33}}(W + i) \not\perp_N; q i e^{i \delta_{33}(W)}; \quad (138)$$

with the invariant energy  $W = \sqrt{1 - q^2} + \epsilon_N^{nr}(q)$ . In detail, one obtains

$$\tan \delta_{33}(W) = \frac{\frac{1}{2} \frac{W}{M} \delta(W)}{W - M \delta(W)} \quad (139)$$

with the width

$$\delta(W) = 2 = m h j (W + i) j i; \quad (140)$$

and mass

$$M(W) = M^0 + \epsilon h j (W + i) j i; \quad (141)$$

Using (130), one obtains explicitly

$$\delta(W) = \begin{cases} \frac{1}{6} \frac{q^3 M_N}{(q) + M_N} - \frac{f_N^0}{m} \frac{2}{F_N^2(q^2)} & \text{for } W > m + M_N; \\ 0 & \text{for } W < m + M_N; \end{cases} \quad (142)$$

and

$$M(W) = M^0 + \frac{4}{3} \int_0^{\frac{W}{m}} \frac{dq^0 q^{04}}{(2^3 2!) (q^0)} - \frac{f_N^0}{m} \frac{2}{W} \frac{F_N^2(q^2)}{(\epsilon_N^{nr}(q^0))} : \quad (143)$$

For the free parameters  $f_N^0$ ,  $m_N$  and  $M^0$ , our fit to the solution SM 95 of [31] yields

$$\frac{f_N^0}{4}^2 = 0.9452; \quad N = 482.11 \text{ MeV}; \quad M^0 = 1281.7 \text{ MeV} \quad n = 2; \quad (144)$$

whereas in [13,19]

$$\frac{f_N^0}{4}^2 = 1.393; \quad N = 287.9 \text{ MeV}; \quad M^0 = 1315 \text{ MeV} \quad n = 1 \quad (145)$$

has been used. We would like to emphasize that the values in (144) have been obtained by fitting simultaneously N scattering in the  $P_{33}$  channel and the  $M_{1+}(\frac{3}{2})$  multipole of photopion production. The reason for this procedure will become apparent in a forthcoming paper on  $\pi^+$  reactions on the deuteron, because it turned out that a reasonable description of the most important  $M_{1+}(\frac{3}{2})$  multipole in the region is not possible in our approach if only N scattering is considered for the  $t$  off  $f_N^0$ ,  $N$  and  $M^0$ .

### C. The transition interaction $NN \rightarrow N$ and $N \rightarrow N$

The transitions  $N \rightarrow NN$  and  $N \rightarrow N$  are generated by the corresponding interaction components of (65) which are depicted in Fig. 8. Similar to [19,20], we restrict ourselves to and exchange. Because we take only  $V^0$  nonvanishing (see Sect. IIIB), only exchange contributes to the three time-ordered diagrams (a) through (c) of Fig. 8. According to the previous discussions, one has to distinguish retarded and static approaches.

Only in the retarded approach, the term  $V_{Px}^0 G^X(z) V_{xP}^0$  in (65) comprises all three time-ordered diagrams (a) through (c) of Fig. 8. The exchange contributions to the other three diagrams (d) through (f) in Fig. 8 have to be described by  $V_N^{0[2]}$ ,  $V_N^{0[2]}$  and  $V_N^{0[2]}$  in view of the truncation of the model Hilbert space, in which no meson-N or meson- $\pi$  configurations are allowed explicitly. In order to have a hermitian interaction, these contributions have to be treated in the energy-independent limit, represented by the diagrams (d') through (f') in Fig. 8 (see the discussion below).

The corresponding matrix elements for exchange have the following structure in the cm. system

$$hN N; p^0 j V_{Nx}^0 G_0(z) V_x^0 \rightarrow N; pi = F(\vec{q}^2) F_N(\vec{q}^2) \frac{f^0 f_N^0}{m^2} \frac{\sim_{NN}(1) \sim_N(2)}{(2)^3 2! (q)} \frac{(\sim_{NN}(1) \sim_N(2) \vec{q}) (\sim_N(2) \vec{q})}{z e_N^{nr}(p) e_N^{nr}(p^0) ! (q)} + (1 \leftrightarrow 2); \quad (146)$$

$$hN N; p^0 j V_x^0 G_0(z) V_x^0 \rightarrow N; pi = F_N^2(\vec{q}^2) \frac{f_N^0}{m^2} \frac{\sim_N(1) \sim_N(2)}{(2)^3 2! (q)} \frac{(\sim_N(1) \sim_N(2) \vec{q}) (\sim_N(2) \vec{q})}{z e_N^{nr}(p) e_N^{nr}(p^0) ! (q)} + (1 \leftrightarrow 2); \quad (147)$$

where  $q = p^0 - p$ . For the evaluation of these expressions, the nonrelativistic reduction of the N vertex has been used and (130). As in (143), we take the nonrelativistic nucleon energies  $e_N^{nr}(p)$  in the NN propagators for simplicity.

The remaining one-pion exchange diagrams (d') through (f') in Fig. 8 and the energy independent limit of all exchange diagrams corresponding to (a) through (f) in Fig. 8 are included in  $V_N^{0[2]}$ ,  $V_N^{0[2]}$  and  $V_N^{0[2]}$ , respectively, which we decompose into and exchange parts according to

$$V_N^{0[2]}(z) = V_N^{0[1]}(z) + V_N^{0[1]}(z); \quad (148)$$

$$V_N^{0[2]}(z) = V^{0[1]}(z) + V^{0[1]}(z); \quad (149)$$

Explicitly, we take for the retarded approach the following expressions

$$hN N; p^0 j V_N^{0[1]} N; pi = F(\vec{q}^2) F_N(\vec{q}^2) \frac{f^0 f_N^0}{m^2} \frac{\sim_{NN}(1) \sim_N(2)}{(2)^3 2! (q)} \frac{(\sim_{NN}(1) \sim_N(2) \vec{q}) (\sim_N(2) \vec{q})}{M_N M^0 ! (q)} + (1 \leftrightarrow 2); \quad (150)$$

$$hN N; p^0 j V_N^{0[1]} N; pi = F_N^2(\vec{q}^2) \frac{f_N^0}{m^2} \frac{\sim_N(1) \sim_N(2)}{(2)^3 2! (q)} \frac{(\sim_N(1) \sim_N(2) \vec{q}) (\sim_N(2) \vec{q})}{2M_N 2M^0 ! (q)} + (1 \leftrightarrow 2); \quad (151)$$

Here we have kept the  $N$  mass difference, which thus is beyond the usual static limit where the mass difference is neglected. The form factor  $F_N$ , parameterized as in (132) with parameters  $\alpha_N$  and  $n$ , and the coupling constant  $f_N^0$  are not identical with  $F_N$  and  $f_N^0$ , respectively, which were fixed by fitting  $N$  scattering data, where configurations are not considered. Consequently,  $F_N$  and  $f_N^0$  can be treated as free parameters to be fixed by  $NN$  scattering (see the following section).

Now, we turn to exchange. Besides the usual  $N$  interaction density [17]

$$i\frac{f_N^0}{m} \tilde{\psi}_N \sim_N \bar{\psi} \sim \bar{\psi} + \text{h.c.}; \quad (152)$$

where  $\tilde{\psi}$ ,  $\bar{\psi}$ , and  $\sim$  denote the Rarita-Schwinger spinor, the nucleon Dirac spinor, and the meson field, respectively, we have considered an additional alternative

$$\frac{g_N^0}{4M_N^2} \tilde{\psi}_N \sim_N (\bar{\psi}) \bar{\psi} \sim \bar{\psi} + \text{h.c.}; \quad (153)$$

which, to our knowledge, has not been discussed in the literature. Using a nonrelativistic reduction of the occurring vertices, we obtain in the cm. frame

$$\begin{aligned} hN N ; p^0 \bar{\psi}_N \tilde{\psi}_N ; p \bar{i} = & \frac{\sim_{NN} (1) \tilde{\psi}_N (2)}{(2)^3 2! (q)} \frac{1}{M_N M^0 \frac{1}{(q)} ! (q)} \frac{1}{! (q)} \\ & F(\bar{q}^2) F_N(\bar{q}^2) \frac{f_N^0}{m} - \frac{g^0}{2M_N} 4i \sim_N (2) \bar{q} \bar{P} \\ & + \frac{g^0 + f^0}{2M_N} (\sim_{NN} (1) \bar{q}) (\sim_N (2) \bar{q}) \\ & + \frac{g^0}{2M_N} \sim_N (\sim_{NN} (2) \bar{q}) (\sim_N (2) \bar{q}) + (1 \pm 2); \end{aligned} \quad (154)$$

$$h N ; p^0 \bar{\psi}^0 \tilde{\psi}^0 j_N ; p \bar{i} = \frac{f_N^0}{m^2} \frac{\sim_N (1) \tilde{\psi}_N (2)}{(2)^3 2! (q)} \frac{1}{2M_N 2M^0 \frac{1}{(q)} ! (q)} \frac{1}{! (q)} \\ F_N^2(\bar{q}^2) (\sim_N (1) \bar{q}) (\sim_N (2) \bar{q}) + (1 \pm 2) \quad (155)$$

with

$$\bar{q} = p^0 - \bar{p}; \quad \bar{P} = \frac{1}{2} (p^0 + \bar{p}); \quad (156)$$

and

$$\sim_N = 1 - \frac{m}{4M_N} \frac{g_N^0}{f_N^0}; \quad (157)$$

Again the form factor  $F_N(\bar{q}^2)$  and coupling constant  $f_N^0$  are fitted to  $NN$  scattering, whereas  $f^0$  and  $g^0$  are fixed by the values of the  $E$  later potential. Note that the terms proportional to  $(\bar{q} \bar{P})$  and  $(\sim_{NN} (2) \bar{q}) (\sim_N (2) \bar{q})$  are usually neglected in the literature, for example in [19,20].

Finally, with respect to the static approach, only the  $N$  potential (147), represented by the diagram (c) in Fig. 8, is generated by iteration of the  $N$  vertex, as has already been mentioned above. All other diagrams of Fig. 8 have to be described by  $V_{PP}^0$  [2] where in addition the  $N - m$  ass difference is neglected. Consequently, we obtain in this limit

$$hN N ; p^0 \bar{\psi}_N \tilde{\psi}_N ; p \bar{i} = F(\bar{q}^2) F_N(\bar{q}^2) \frac{f^0 f_N^0}{m^2} \frac{\sim_{NN} (1) \tilde{\psi}_N (2)}{(2)^3 !^2 (q)} \\ (\sim_{NN} (1) \bar{q}) (\tilde{\psi}_N (2) \bar{q}) + (1 \pm 2); \quad (158)$$

whereas Eqs. (151), (154), and (155) apply also to the static limit except for the neglect of the  $N - m$  ass difference. Note however, that in this case all coupling constants and cut-offs in  $V_N^0$  and  $V^0$  can be treated as free parameters due to the choice  $V_{NN}^0 = 0$ .

## D . The interaction $V_{XX}^0$

The simplest choice for the diagonal interaction in the subspace  $H_{NNN}^{[2]}$  would certainly be  $V_{XX}^0 = 0$ . However, such a choice would lead to severe inconsistencies with respect to d.o.f., because it would lead to a violation of three-body unitarity. The reason for this violation lies in the fact that for excitation energies up to about 500 MeV,  $N\bar{N}$  and  $d$  states can exist in this sector as asymptotic free states (energetically allowed 2 and 3 states are forbidden due to the one-meson approximation). The corresponding asymptotic scattering states  $j_{NNi}$  and  $j_{di}$  obey the equations

$$H_0, j_{NNi} = E_{NN} j_{NNi}; \quad (159)$$

$$(H_0, + V^0) j_{di} = E_d j_{di}; \quad (160)$$

It is therefore obvious, that the interaction  $V^0$ , which describes the  $NN$  interaction in the presence of a non-interacting pion, must be considered at least in the  $^3S_1-^3D_1$  channel which we will henceforth refer to as the  $d$  channel. Otherwise, the  $d$  state would not be present formally, so that reactions like  $d + d \rightarrow d + d$  cannot be studied without creating inconsistencies. In [21-23], for example, reactions with a  $d$  state in the initial and/or final state were studied without considering  $V^0$ . Consequently, unitarity is violated above the  $d$  threshold, since the imaginary part of the forward  $NN$  scattering amplitude would be connected with the total cross sections of the reactions  $NN \rightarrow NN$  and  $NN \rightarrow NN$  only. On the other hand, the contribution of  $NN \rightarrow d + d$  cannot be taken into account if  $V^0 = 0$ . Therefore,  $V^0$  has to be considered nonzero, since we are interested in the construction of an unitary model up to the  $d$  threshold. All other diagonal interactions in  $H_{NNN}^{[2]}$  do not affect three-body unitarity for energies up to 500 MeV and, therefore, can safely be set equal to zero for the sake of simplicity (see (35) and (36)). We consider this choice as the minimal requirement in order to satisfy three-body unitarity.

Thus we retain in  $V_{XX}^0$  solely the interaction of two nucleons with isospin  $t=0$  in the presence of a pion as spectator, where we restrict ourselves to an interaction, called  $V^d$ , which acts only in the  $^3S_1-^3D_1$  channel. Then  $V_{XX}^0$  can be written in the form (see Fig. 9)

$$V_{XX}^0 = \frac{Z}{(2\pi)^3 2!} \int \frac{d^3 q}{(q)} j_{(q)} i V^d (M_d + \frac{q^2}{4M_N}) h_{(q)} j; \quad (161)$$

where  $j_{(q)} i$  denotes the spectator pion state with momentum  $q$ . For practical reasons, we use for  $V^d$  a separable interaction of rank 1

$$V^d(\omega) = \frac{G_0^{-1}(\omega) j_{di} h_{di} j G_0^{-1}(\omega)}{h_{di} G_0^{-1}(\omega) j_{di}}; \quad (162)$$

which satisfies the Schrödinger equation for the nucleonic component of the deuteron

$$H_0 + V^d(M_d) - M_d j_{di} = 0; \quad (163)$$

or in equivalent form

$$(G_0(M_d) V^d(M_d) - 1) j_{di} = 0; \quad (164)$$

The separable structure of  $V^d$  leads to a rather simple expression for the relevant amplitude  $T^d$  of (62). One obtains

$$T^d(z) = \frac{Z}{(2\pi)^3 2!} \int \frac{d^3 q}{(q)} j_{(q)} i T^d(M_d + \frac{q^2}{4M_N}; z - \frac{q^2}{4M_N}) - !_{(q)} h_{(q)} j; \quad (165)$$

where the auxiliary amplitude  $T^d$ , satisfying the Lippmann-Schwinger equation

$$T^d(\omega; z) = V^d(\omega) + V^d(\omega) G_0(z) T^d(\omega; z); \quad (166)$$

is given by the analytic expression

$$T^d(\omega; z) = \frac{G_0^{-1}(\omega) j_{di} h_{di} j G_0^{-1}(\omega)}{h_{di} G_0^{-1}(\omega) j_{di} h_{di} G_0^{-1}(\omega) G_0(z) G_0^{-1}(\omega) j_{di}}; \quad (167)$$

The shifted arguments in  $T^d$  in (165) have their origin in the fact that the two nucleons interacting via  $V^d$  have total momentum  $q$ . We use the nonrelativistic energy in order to separate the c.m. energy exactly. It is therefore

natural to use the nonrelativistic energy also in the propagator  $G_0$  in (167). Boost contributions to the deuteron wave function are expected to be small [32] and thus are neglected. In our numerical evaluation the intermediate  $NN$  propagation, entering into the term  $V_{pX}^0 G_0(z) T^X(z) G_0(z) V_{Xp}^0$  [con (cut A and B in Fig. 9) of Eq. (65)] is treated in the static limit for simplicity. Moreover, we use for the  $N$  vertex  $V_{Np}^0$  in  $V_{pX}^0 G_0(z) T^X(z) G_0(z) V_{Xp}^0$  the nonrelativistic version. Both approximations lead to a slight violation of unitarity which, however, is not critical.

At the end of this subsection, we will discuss briefly the quality of the separable interaction in the  $^3S_1$ - $^3D_1$  channel. For the deuteron pole, i.e., for  $W = M_d$ , the resulting amplitude  $T^d$  is identical to the exact solution obtained with the Bonn-OBEPF and Elster-potentials, respectively. However, for  $W \neq M_d$  this equivalence breaks down. Concerning the resulting phase shifts, one obtains a strong deviation from the exact calculation for the  $^3D_1$  phase shift and the mixing parameter (see Fig. 10)). The most important  $^3S_1$  channel, however, is described reasonably well. These facts indicate the limits of the separable ansatz.

#### E. The problem of double counting

Before discussing the nucleon-nucleon interaction, we would like to focus first on the important issue of double counting and how it can be avoided by a renormalization procedure. The problem of double counting appears if one starts from an operator taking into account effectively certain d.o.f., which have been projected out before but which are introduced later on again explicitly. For example, let us consider a realistic  $NN$  potential like Bonn-OBEPF, Bonn-OBEPQ [4,17], Paris [30], Argonne V<sub>14</sub> [33], or Nijmegen [34]. These potentials act in pure nucleonic space and do not consider the isobar explicitly, because they are fitted to deuteron properties and  $NN$  scattering data below threshold, where d.o.f. are less important. However, if such potentials are used in a model with explicit d.o.f. in addition within a coupled channel approach, the problem of double counting becomes evident, because, for example, the dispersive box graphs depicted in Fig. 11 would be considered in addition explicitly.

A simple way out of this problem is the so-called box renormalization of Green and Sainio [35] which consists in a subtraction of the box diagrams at a fixed energy  $E_0$  from  $V_{NN}^{0;\text{con}}$  in (65). We will adopt this method also here and use [similar to previous work [13,18{20,23] [the value  $E_0 = 2M_N$ . With respect to the above discussion we will distinguish

(i) static calculations ( $V_{Np}^0 = 0$ ):

$$V_{NN}^{0[2]} = V_{NN}^{\text{real}} - V_N^0 G_0(z) V_N^0 \Big|_{z=E_0} - V_{Np}^0 G_0(z) T^X(z) G_0(z) V_{Xp}^0 \Big|_{z=E_0}; \quad (168)$$

and

(ii) retarded calculations ( $V_{Np}^0 \neq 0, V_{NN}^{\text{real}} = 0$ ):

$$V_{NN}^{0[2]} = V_N^{0\text{full}}(z) G_0(z) V_N^{0\text{full}}(z) \Big|_{z=E_0} - V_{Np}^0 G_0(z) T^X(z) G_0(z) V_{Xp}^0 \Big|_{z=E_0}; \quad (169)$$

where we have defined

$$V_N^{0\text{full}}(z) = V_N^0(z) + V_{Np}^0 G_0(z) V_{Xp}^0 \Big|_{\text{con}}; \quad (170)$$

It should be emphasized that the intermediate  $N$  and  $d$  states have isospin  $t = 1$  so that the box subtraction has no influence on the ( $t = 0$ ) channels, especially for the deuteron. However, such a subtraction would appear if also configurations would be included explicitly. Finally, we would like to remark that the inclusion of (169) in the Lippmann-Schwinger equation (88) leads to an energy dependence of the subtracted box graphs which can be avoided by the substitution

$$\hat{R}(z) V_{NN}^{0[2]} \hat{R}(z) - f \hat{R}(z) V_{NN}^{0[2]} \hat{R}(z) g \Big|_{z=E_0} \quad (171)$$

in the driving term  $\hat{R}(z) V_{pp}^{\text{con}}(z) \hat{R}(z)$  of (88).

#### F. The nucleon-nucleon interaction

The properties of the two-nucleon system is governed by the  $NN$  interaction. In this work, we restrict ourselves to realistic  $NN$  potentials known from the literature, which have to be renormalized according to the discussion in the foregoing subsection if additional degrees of freedom are considered explicitly like, e.g., and  $d$ .

The starting points of our considerations are the Lippmann-Schwinger equation for the  $N\bar{N}$  scattering matrix (88) and the Schrödinger equation for the effective, purely nucleonic component of the deuteron (115), which we write in the form  $s$ , respectively,

$$T_{NN}^{\text{con}}(z) = V_{NN}^{\text{eff}}(z) + V_{NN}^{\text{eff}}(z)G_0(z)T_{NN}^{\text{con}}(z); \quad (172)$$

$$H_0 + V_{NN}^{\text{eff}}(M_d) \not{p}_i = M_d \not{p}_i \quad (173)$$

with the effective  $N\bar{N}$  interaction

$$V_{NN}^{\text{eff}}(z) = \not{P}(z) V_{NN}^{[2]} + V_{N\bar{N}} G_0(z) V_{N\bar{N}} l_{\text{con}} \not{P}(z); \quad (174)$$

Note that in (172) the isobar and the  $d$  channel has been neglected, because the realistic  $N\bar{N}$  potential models do not consider these additional degrees of freedom in general. Exceptions are, for example, the "full" Bonn and the Argonne  $V_{28}$  potentials [17,33] which include the  $d$ .

In view of the discussion in the foregoing subsection, we follow different strategies in static and retarded calculations. In the static limit the effective interaction simplifies to

$$V_{NN}^{\text{eff}}(z) = V_{NN}^{[2]}; \quad (175)$$

for which we use the Bonn-OBEPF potential  $V^{\text{OBEPF}}$  [17] to be renormalized according to Eq. (168), whereas in the retarded approach  $V_{NN}^{[2]}$  in  $V_{NN}^{\text{eff}}(z)$  has to be chosen as (cf. (169)):

$$\begin{aligned} V_{NN}^{[2]} &= (\not{P}_{[2]}^{\text{pos}})^{-1} V_{NN}^{[0]} (\not{P}_{[2]}^{\text{pos}})^{-1} \\ &= V_{N\bar{N}}(z) G_0(z) V_{N\bar{N}}(z)_{z=2M_N} V_{N\bar{N}} G_0(z) T^X(z) G_0(z) V_{N\bar{N}}(z)_{z=2M_N}; \end{aligned} \quad (176)$$

with

$$V_{N\bar{N}} = \not{P}_{[2]}^{\text{pos}} V_N^{\text{full}} (\not{P}_{[2]}^{\text{pos}})^{-1} \quad (177)$$

(note the analogy to (85) and (86)). Concerning the one-boson exchange part in (174), we are able to use the potential model  $V^{\text{Elster}}$  of Elster et al. [28,29], which can be considered as an extension of the retarded Bonn-OBEPF potential [17] with respect to the inclusion of additional  $N$  loops. Consequently, we use in the retarded calculations (note (171))

$$V_{NN}^{\text{eff}}(z) = V^{\text{Elster}}(z) + \not{P}(z) V_{NN}^{[2]} \not{P}(z)_{z=2M_N}; \quad (178)$$

where  $V_{NN}^{[2]}$  is given by (176), and the pionic part  $\not{P}(z)$  of the dressing factor is discussed below.

Because of its importance for the present work, it is worthwhile to study  $V^{\text{Elster}}$  in some more detail. Concerning the one-boson exchange, all six mesons  $\pi$ ,  $\rho$ ,  $\omega$ ,  $\rho'$ ,  $\omega'$  and  $\rho''$  are taken into account whereas only the pion is considered in the dressing operator, therefore denoted by  $\not{P}(z)$ , for simplicity. This approximation is, however, not crucial with respect to unitarity up to the threshold. Consequently,  $V^{\text{Elster}}(z)$  has the structure

$$V^{\text{Elster}}(z) = \not{P}(z) \sum_{\text{xf}, \pi, \rho, \omega, \rho', \omega'}^X V_{N\bar{N}} G_0(z) V_{N\bar{N}} l_{\text{con}} \not{P}(z); \quad (179)$$

where  $\not{P}(z)$  is given in analogy to (84) with only  $N$  loops in  $\not{P}_{[2]}(z)$ . Explicitly, one obtains for the matrix element of the latter using the  $N$  vertex of (125)

$$hN\bar{N}; \not{p}^0 \not{P}_{[2]}(z) \not{N}\bar{N}; \not{p}_i = (\not{p}^0 - \not{p}) Z_{[2]}(z; \not{p}) \quad (180)$$

with

$$\begin{aligned} Z_{[2]}(z; \not{p})^2 &= 1 + 2 \frac{g^0}{4} \frac{3}{4} \frac{Z_1}{\int_0^{\infty} dk \frac{k^2}{\epsilon_N(k)}} \frac{Z_1}{\int_1^{\infty} dk \cos F^2((\not{p} - \not{k})^2)} \\ &\quad \frac{\epsilon_N(\not{p}) \epsilon_N(k)}{M_N^2} \frac{pk \cos}{!(\not{p} - \not{k}) \epsilon_N(\not{p}) \epsilon_N(k) - !(\not{p} - \not{k}) z \epsilon_N(k) - !(\not{p} - \not{k})}; \end{aligned} \quad (181)$$

where the the angle between  $\mathbf{p}$  and  $\mathbf{k}$  is denoted by  $\theta$ .

In view of the renormalization of  $V_{N\bar{N}}^0$  by the operator  $\frac{p_{[2]}^{\text{bos}}}{2}$ , renormalized coupling constants

$$f_x = \frac{f_x^0}{\frac{p_{[2]}^{\text{bos}}}{2}}; \quad x \text{ } 2 \text{ } f!; \text{ } g; \quad (182)$$

$$g_x = \frac{g_x^0}{\frac{p_{[2]}^{\text{bos}}}{2}}; \quad x \text{ } 2 \text{ } f; \text{ } ; \text{ } ; \text{ } ; \text{ } !; \text{ } g \quad (183)$$

will appear in (179), whose energy dependence due to  $\frac{p_{[2]}^{\text{bos}}}{2}$  is small and therefore can be neglected (see Fig. 12). The free parameters in (179), i.e., the cut-offs and physical coupling constants are fixed by fitting  $N\bar{N}$  scattering data below threshold and deuteron properties. The resulting values are presented in Table I.

#### IV. RESULTS FOR $N\bar{N}$ SCATTERING

##### A. Determination of the parameters

We now will consider  $N\bar{N}$  scattering in order to fix the remaining free parameters in the hadronic interaction. As discussed in Sect. III C, in a retarded approach the parameters of the diagrams (a) through (c) of Fig. 8 are in principle fixed by the parametrization of the meson-nucleon vertices (Sect. III A) and of the  $N$  vertex  $V_N^0$  (Sect. III B). Consequently, only the cut-offs and coupling constants in the diagrams (d') through (f') can be treated as free parameters. According to (148) through (155), these diagrams contain five open parameters, namely the coupling constants  $f_N^0$  and  $f_{N\bar{N}}^0$ , the parameter  $\mu_N$  (157) and the form factors  $F_N(q^2)$  and  $F_{N\bar{N}}(q^2)$  which are parametrized as in (128). However, the question arises whether the parametrization of the  $N$  vertex as obtained from fitting  $N$  scattering data should be used for the OBE mechanisms, too. For example, one of the differences between  $N\bar{N}$  and  $N$  scattering is the fact that in  $N\bar{N}$  scattering above threshold a pion can be onshell, whereas in  $N$  scattering it must be onshell. This leads to dramatic differences in the cut-off  $\mu_N$  in (132). For example, the value of 1200 MeV (with  $n = 1$ ) for  $\mu_N$  in the full Bonn potential [17] is much stronger than the value of typically 300 MeV ( $n = 1$ ) or 500 MeV ( $n = 2$ ) obtained from  $N$  scattering. Similar differences do occur also for the parametrization of the  $N$  vertex in  $N\bar{N}$  versus  $N$  scattering.

Holzwarth and Machleidt [36] have shown in a detailed analysis that these problems can be traced back to the use of the monopole or dipole parametrization of the hadronic form factors, which ties together the low and high momentum behaviour and thus is not able to describe both  $N\bar{N}$  and  $N$  data simultaneously with the same cut-off. In  $N\bar{N}$  scattering, for example, pion momenta in the neighbourhood of  $q = 0$  are the relevant ones. Thus for small  $q$ , the form factor should be close to one in order to achieve, for example, a quantitative description of the deuteron quadrupole moment, which is dominated by long-range mechanisms. Therefore, a large cut-off mass is needed. On the other hand, for large cut-off masses the form factor does not decrease fast enough with increasing pion momenta as is necessary in  $N$  scattering. However, a form factor which is derived from the Skyrme model is able to describe both,  $N\bar{N}$  as well as  $N$  scattering, simultaneously [36], because it combines the features of a hard monopole or dipole form factor at  $q = 0$  with the quality of a soft form factor for larger pion momenta.

For these reasons (although we are aware of the fact that this procedure leads to additional inconsistencies (e.g., violation of unitarity)), we do not use the values (144) in the OBE mechanism of our coupled  $N\bar{N}$ - $N$  system. Thus, we replace the coupling constant  $f_N^0$  and the form factor  $F_N(q^2)$  in the retarded diagrams (a) and (b) of Fig. 8 (see (146)) by the corresponding quantities  $f_N^0(q^2)$  and  $F_N(q^2)$  of diagram (d') and (e'), respectively. For the  $N \rightarrow N$  transition (diagrams (c) and (f') in Fig. 8) we use the values (144) or (145) as obtained from  $N$  scattering. Similar to previous studies [13,37], we do not determine the free parameters by a global fit to all  $N\bar{N}$  channels in the region. Instead, we concentrate on the most important  $^1D_2$  channel, because it is the only partial wave which couples to a  $N \rightarrow S$  state (see Table II).

We begin with the discussion of the parameter choices for the retarded approach as listed in Table III. For  $f_N^0$ ,  $f_{N\bar{N}}^0$ , and the cut-off  $\mu_N$ , we have chosen the values of the full Bonn Potential, i.e.,

$$\frac{f_N^0}{4}^2 = 0.224; \quad \frac{f_{N\bar{N}}^0}{4}^2 = 20.45; \quad \mu_N(q^2) = 1200 \text{ MeV}; \quad n = 1; \quad (184)$$

It turned out that for a variety of different combinations of the remaining parameters  $\mu_N$  and  $n$  a satisfactory description of the  $^1D_2$  phase shift is possible. Thus we have restricted the choice of  $\mu_N$  to the values  $\mu_N =$

$1; 0; 1$ . The resulting cut-off masses  $N$  are listed in Table III as determined by a fit to the  $^1D_2$  phase shift at  $T_{\text{lab}} = 500$  MeV.

The value  $N = 1$  corresponds to the usual neglect of the additional coupling (153). On the other hand, the choice  $N = 0$  can be motivated by vector dominance insofar as for this choice the  $N$  vertex has the same spin structure as the  $N$  coupling, which consists in general of an electromagnetic M 1 and E 2 excitation, provided one neglects the small E 2 transition.

As next, we turn to the static case. We would like to remind the reader that in this case all diagrams except the contribution (f) of Fig. 8 are incorporated into the static part of  $V^0$  [2], where all corresponding coupling constants ( $f^0, f^0, g^0, f_N^0, f_N^0$ ), the parameter  $N$  and all form factors  $F, F_N$  and  $F_N$  are treated as free parameters. The resulting values are listed in Table IV. In the simplest approach, CC (stat1, ), which is identical to the one used in [13], we neglect the d channel and the exchange in  $V_N^0$  and  $V^0$  completely, e.g., the  $N$  interaction is solely given by a exchange, where the cut-off  $N_N = N$  is fitted to the  $^1D_2$  partial wave at  $T_{\text{lab}} = 500$  MeV. The  $N$  vertex  $V^0$  is given by the parametrization (145) of Sauer et al. [19]. Similar to the retarded case, we use these parameters (145) also in the potential  $V^0$  (diagram (f) of Fig. 8).

The second approach CC (stat2, ) differs from CC (stat1, ) only with respect to the parametrization (144) instead of (145) for  $V^0$ , e.g., those values for  $V^0$  are taken into account which are also present in our retarded approach. The choice (144) is also used in our third choice CC (stat, ; ; 0). But in contrast to the previous cases, we incorporate in addition exchange in  $V_N^0$  and  $V^0$  as well as the d channel. Furthermore, we set  $N = 0$ .

## B. Results

We will first consider the results for the retarded approach. It turns out that all three retarded potential models are able to describe phase shift and inelasticity in the  $^1D_2$  channel equally well, see Fig. 13. This is of course not very surprising because we use this channel for fixing the free parameters. However, one should note the rather large discrepancies between theory and experiment [31] in the phase shift for energies  $T_{\text{lab}} = 800$  MeV. With respect to the other channels, one observes a surprisingly large dependence of the P waves on  $N$  (see Fig. 14). However, it is not possible to determine an optimal value for  $N$ . While the  $^3P_0$  inelasticity and the  $^3P_1$  channel seem to favour  $N = 1$ , the value  $N = 1$  leads to a slightly better fit of the  $^3P_2$  channel, especially for energies  $T_{\text{lab}} = 700$  MeV. The overall description is still quite poor. This rather unsatisfactory situation is, however, not very surprising since we have not fitted our parameters to all partial waves simultaneously.

For the further discussion we have chosen the model CC (ret, ; ; 0) as a starting point and compare it with the static approaches CC (stat1, ), CC (stat2, ), and CC (stat, ; ; 0) for all ( $t = 1$ ) partial waves with total angular momentum  $j = 3$  as shown in Figs. 15 through 17. With respect to the  $^1D_2$  phase shift, all four models yield more or less similar results. The inelasticity in CC (stat1, ) and CC (stat2, ), however, is somewhat smaller than in the other two models. In accordance with [38], this behaviour can be traced back to the neglect of the d channel in CC (stat1, ) and CC (stat2, ). For the other partial waves, the comparison with experimental data does not give a uniform picture. For example, the calculation CC (stat, ; ; 0) yields the comparably best, but still not satisfactory description of the  $^3P_1$  phase shift and the  $^3P_0$  inelasticity. On the other hand, the theoretical  $^3P_2$  phase shift is largely at variance with the data, whereas CC (stat1, ) and CC (stat2, ) result in a rather good description. But in the  $^1S_0$  and the  $^3F_3$  channels the retarded calculation CC (ret, ; ; 0) is favoured.

In summary, one finds that our fit procedure leads to a satisfactory agreement with the experimental data for the  $^1D_2$  channel, which is the most important one in the resonance region. The overall description of the other channels is fairly well but needs further improvements. As a first step one would need to construct a potential model within our approach (static or retarded) where all parameters are fixed simultaneously to all partial waves for energies up to about  $T_{\text{lab}} = 1$  GeV. This quite involved task will be one of our future projects.

Another remark is in order with respect to the question whether the static or the retarded interaction gives a better description. Although in principle, from the basic physical ideas, a retarded interaction is more appropriate, our results for the pure hadronic reactions do not allow a clear cut distinction which one is better. To this end, one has to consider e.m. reactions where first results [14,15] indicate a preference for the retarded interaction. This will be elaborated in greater detail in forthcoming papers.

## C. Comparison with other theoretical approaches

In the coupled  $N\bar{N} \rightarrow N\bar{N}$  approach of Leidemann et al. [12], the static Reid soft core and Argonne potentials have been used as starting point for the  $N\bar{N}$  interaction, whereas the d channel has been neglected. Since the numerical

calculations have been performed in  $r$ -space, non localities, which are, for example, present in the  $N$  propagation, could not be taken into account exactly. Therefore, additional approximations in the renormalization procedure had been used which lead to a much more flexible treatment by introducing one additional free parameter for each  $NN$  channel. Thus, compared with our results, a better description of the  $NN$  scattering data was achieved because of this additional phenomenological ingredient.

A retarded interaction in a coupled channel calculation with an explicit  $N$  vertex has been used by Bulla et al. [20]. However, this work contains at least two important differences compared to our approach: (i) Retardation is treated only for pion exchange. For the cut-off mass of the corresponding  $N$  vertex form factor, a very small value of 443 MeV has been used in dipole parametrization which has been obtained from a fit of  $N$  scattering data in the  $P_{11}$  channel, whereas the value of 1700 MeV in the Elster potential is a result of a fit to  $NN$  scattering data. (ii) The static Paris potential is used as the underlying  $NN$  interaction. Therefore, in view of the renormalization procedure (123), the effective retarded OPE potential is considerably weakened. In view of these differences, it is not very surprising that Bulla et al. found only a small influence of retardation, in fact much smaller than in our approach.

Finally, we would like to mention the work of Wilbois [37]. Among other things, he compared the results of a coupled channel approach for different static  $NN$  potentials (Bonn OBEP, Bonn OBEPQ, Paris and Nijmegen). It turned out that the  $NN$  phase shifts and inelasticities are rather sensitive to the choice of the underlying  $NN$  potential. Similar to our result, a satisfactory description of the whole experimental data set could not be achieved.

#### V. SUMMARY AND OUTLOOK

In this paper, we have presented the hadronic part of a model which is suited for the study of electromagnetic and hadronic reactions in the two-nucleon sector, for example,  $NN$  scattering or electromagnetic deuteron break-up, up to about 500 MeV excitation energy, in which not more than one pion is created or absorbed. This model respects in particular three-body unitarity. It is based on a previously developed model of Sauer and collaborators [18{20] which allows the explicit consideration of retardation in the two-body meson-exchange operators within a  $NN$ - $N$  coupled channel approach using time-ordered perturbation theory.

Since retarded interactions are not hermitean, we have generated the retarded one-boson exchange mechanisms by considering explicitly meson-nucleon and  $N$  vertices. Therefore, additional mesonic degrees of freedom beside the baryonic components had to be included explicitly into the Hilbert space of a two-baryon system. In the present work, we have restricted ourselves to the one-meson approximation, which means that we allow only configurations with one meson present besides the baryons. As mesons we have taken into account explicitly ; ; ; , and . In order to satisfy two- and three-body unitarity, we have incorporated the  $d$  channel as well as intermediate pion-nucleon loops. In view of the latter mechanism, a distinction between bare and physical nucleons was necessary in order to avoid inconsistencies.

In our explicit realization within a field-theoretical framework, we have used the realistic retarded potential model of Elster et al. [28,29] as input for the basic nucleon-nucleon interaction in pure nucleonic space. This potential had to be renormalized because of the additional d.o.f., which lead to additional contributions from  $N$  and  $d$  states. Because of some necessary approximations in our numerical evaluations, unitarity is not completely obeyed. The free parameters of our model have been fixed by fitting  $N$  scattering in the  $P_{33}$  channel and  $NN$  scattering in the  $^1D_2$  channel. For practical reasons, no global fit of the parameters to all relevant  $NN$  or  $N$  channels has been performed. Therefore, the overall description of the  $NN$  phase shifts and inelasticities is fairly well but needs some further improvement in the future. The best way for such an improvement would be to construct from scratch a hadronic interaction model which incorporates from the beginning nucleon, meson, and degrees of freedom and whose open parameters are fitted to the phase shifts and inelasticities of all relevant  $NN$  scattering partial waves for  $T_{\text{lab}}$  energies up to about 1 GeV.

However, we believe that the present model is realistic enough for the study of electromagnetic reactions like photo- and electrodisintegration of the deuteron as well as pion production. The reason is that the  $^1D_2$  channel, which is the most important one in such electromagnetic and hadronic reactions in the region, is described reasonably well because of our specific fit of just this partial wave. The predictions for the observables of such reactions will be presented in forthcoming papers.

---

[1] C. Herberg et al., Eur. Phys. Journal A 5, 131 (1999); M. Ostrick et al., Phys. Rev. Lett. 83, 276 (1999).

[2] I. Passchier et al, Phys. Rev. Lett. 82, 4988 (1999).

[3] H. A renhovel, G. K re, R. Schmid, and P. W ilhelm, Phys. Lett. B 407, 1 (1997); Nucl. Phys. A 631, 612c (1998).

[4] R. M achleidt, Adv. Nucl. Phys. Vol. 19, p. 189 (Plenum, New York, 1989).

[5] J. Carlson and R. Schiavilla, Rev. Mod. Phys. 70, 743 (1998).

[6] H. A renhovel and M. Sanzone, Few-Body Syst. Suppl. 3, 1 (1991).

[7] H. A renhovel, Few-Body Syst. 26, 43 (1999).

[8] H. A renhovel, F. Ritz, and Th. W ilbois, nucl-th/9910009.

[9] J.M. Laget, Nucl. Phys. A 312, 265 (1978); Can. J. Phys. 62, 1046 (1984).

[10] M. Schwamb, H. A renhovel, and P. W ilhelm, Few-Body Syst. 19, 121 (1995).

[11] H. Tanabe and K. Ohta, Phys. Rev. C 40, 1905 (1989).

[12] W. Leidemann and H. A renhovel, Nucl. Phys. A 465, 573 (1987).

[13] P. W ilhelm and H. A renhovel, Phys. Lett. B 318, 410 (1993).

[14] M. Schwamb, H. A renhovel, P. W ilhelm, and Th. W ilbois, Phys. Lett. B 420, 255 (1998).

[15] M. Schwamb, H. A renhovel, P. W ilhelm, and Th. W ilbois, Nucl. Phys. A 631, 583c (1998).

[16] M. Schwamb, PhD Thesis, Mainz 1999.

[17] R. M achleidt, K. H olinde, and Ch. Elster, Phys. Rep. 149, 1 (1987).

[18] P. J. Sauer, Progress in Particle and Nuclear Physics, Vol. 16, ed. A. Faessler (Pergamon Press, 1986).

[19] H. P opping, P. J. Sauer, and X. -Z. Zang, Nucl. Phys. A 474, 557 (1987);  
H. P opping, P. J. Sauer, and X. -Z. Zang, Nucl. Phys. A 550, 563 (1992).

[20] A. Bulla and P. J. Sauer, Few-Body Syst. 12, 141 (1992).

[21] M. T. Pena, H. G arcilazo, U. Oelfke, and P. U. Sauer, Phys. Rev. C 45, 1487 (1992).

[22] P. W ilhelm and H. A renhovel, Nucl. Phys. A 593, 435 (1995).

[23] P. W ilhelm and H. A renhovel, Nucl. Phys. A 609, 469 (1996).

[24] P. J. Sauer, M. Sawicki, and S. Furui, Prog. Theor. Phys. 74, 1290 (1985).

[25] A. N. Kvinikhidze and B. B. Blankleider, Phys. Rev. C 48, 25 (1993).

[26] A. N. Kvinikhidze and B. B. Blankleider, Phys. Lett. B 307, 7 (1993).

[27] B. B. Blankleider and A. N. Kvinikhidze, Few-Body Syst. Suppl. 7, 294 (1994).

[28] Ch. Elster, PhD Thesis, Bonn 1986.

[29] Ch. Elster, W. Ferchlander, K. H olinde, D. Schutte, and R. M achleidt, Phys. Rev. C 37, 1647 (1988).

[30] M. Lacombe, B. Loiseau, J. M. Richard, R. V inh M au, J. C ôte, P. P ires, and R. de Tourreil, Phys. Rev. C 21, 861 (1980).

[31] R. A. Amato et al., program SA ID.

[32] H. G oller and H. A renhovel, Few-Body Syst. 13, 117 (1992).

[33] R. B. W iringa, R. A. Sm ith, and T. L. A insworth, Phys. Rev. C 29, 1207 (1984).

[34] V. G. J. Stoks, R. A. M. K lom p, C. P. F. Terheggen, and J. J. de Swart, Phys. Rev. C 49, 2950 (1993).

[35] A. M. G reen and M. E. Sainio, J. Phys. G 8, 1337 (1982).

[36] G. H olzwarth and R. M achleidt, Phys. Rev. C 5, 1088 (1997).

[37] Th. W ilbois, PhD Thesis, Mainz 1996.

[38] H. Tanabe and K. Ohta, Phys. Rev. C 36, 2495 (1987).

#### APPENDIX : THE TWO-POTENTIAL FORMULA

Let us consider the Lippmann-Schwinger equation

$$T(z) = W + W G_0(z) T(z); \quad (185)$$

where the interaction  $W$  can be written as a sum of two terms

$$W = W_1 + W_2; \quad (186)$$

First, we introduce the scattering matrix  $T_1$ , corresponding to the driving term  $W_1$ , which is defined by the integral equation

$$T_1(z) = W_1 + W_1 G_0(z) T_1(z); \quad (187)$$

or equivalently by

$$\begin{aligned} G_1(z) &= (z - H_0 - W_1)^{-1} \\ &= G_0(z) + G_0(z) T_1(z) G_0(z); \end{aligned} \quad (188)$$

Introducing the auxiliary amplitude  $\mathcal{F}(z)$  via

$$\mathbb{P}(z) = W_2 + W_2 G_1(z) \mathbb{P}(z); \quad (189)$$

one obtains by some algebraic manipulations the two-potential formula for the full amplitude  $T(z)$ :

$$T(z) = T_1(z) + [1 + T_1(z)G_0(z)]\mathbb{P}(z) [1 + G_0(z)T_1(z)] \quad (190)$$

or equivalently with the help of (188)

$$T(z) = G_0^{-1}(z) [G_1(z) + G_1(z)\mathbb{P}(z)G_1(z)]G_0^{-1}(z) \quad G_0^{-1}(z); \quad (191)$$

The advantage of the equation (190) compared to (185) is the fact that in the kernel of the first one, the interaction  $W_1$  is completely taken into account by the amplitude  $T_1(z)$ . In practical calculations, the two-potential formula is therefore extremely helpful if  $T_1$  is given in an analytic form, for example, by taking a separable ansatz for  $W_1$ .

TABLE I. Meson parameters of  $V^{\text{Ester}}$ . The parameters for the  $\pi$  boson apply only to the ( $t = 1$ )-NN potential. For  $t = 0$ , we use  $g^2 = 4 = 9.4050$ ,  $m = 580$  MeV,  $\kappa = 2300$  MeV,  $n = 1$ .

$x$	$\frac{g_x^2}{4} (f_x = g_x)$	$m_x$ [MeV]	$\kappa$ [MeV]	$n_x$
!	14.4	138.03	1700	2
	0.9 (6.1)	769	1500	1
	20.0 (0)	782.6	1500	1
	9.4080	575	2600	1
	0.3912	983	1500	1
	5.0	548.8	1500	1

TABLE II. NN and N partial waves ( ${}^{2s+1}l_j$ ) with total angular momentum  $j = 3$ , parity and isospin  $t$ .

$j$	$t$	NN	N
0	+	${}^1S_0$	${}^5D_0$
	1	${}^3P_0$	${}^3P_0$
1	+	${}^3P_1$	${}^3S_1, {}^3D_1, {}^5D_1$
	1	${}^3P_1$	${}^3P_1, {}^5P_1, {}^5F_1$
1	+	${}^3S_1, {}^3D_1$	
	0	${}^1P_1$	
2	+	${}^1D_2$	${}^5S_2, {}^3D_2, {}^5D_2, {}^5G_2$
	1	${}^3P_2, {}^3F_2$	${}^3P_2, {}^5P_2, {}^3F_2, {}^5F_2$
2	+	${}^3D_2$	
	0		${}^3D_3, {}^5D_3, {}^3G_3, {}^5G_3$
3	+	${}^3F_3$	${}^5P_3, {}^3F_3, {}^5F_3, {}^5H_3$
	1	${}^3D_3, {}^3G_3$	
3	+	${}^1F_3$	
	0		

TABLE III. Parameter values for  $V_N^0$  and  $V^0$  in the retarded approach.

CC (type)	$\frac{(f_N^0)^2}{4}$	$N$	$\text{MeV}$	$n$	$\frac{(f_N^0)^2}{4}$	$N$	$\text{MeV}$	$n$	$N$
(ret; ; ; 1)	0.224	1200		1	20.45	1340		2	1
(ret; ; ; 0)	0.224	1200		1	20.45	1420		2	0
(ret; ; ; 1)	0.224	1200		1	20.45	1560		2	1

TABLE IV. Parameter values in the static approach. Note that the models differ in the parametrization of the  $N$  vertex  $V^0$  (see the discussion in the text).

CC (type)	$\frac{(f^0)^2}{4}$	[MeV]	n	$\frac{(f^0)^2}{4} (f^0 = g^0)$	[MeV]	n			
(stat1; )	0.08	700	1	0 (0)					
(stat2; )	0.08	680	1	0 (0)					
(stat; ; ; 0)	0.0778	1300	1	0.84 (6.1)	1400	1			
CC (type)	$\frac{(f^0_N)^2}{4}$	N	[MeV]	n	$\frac{(f^0_N)^2}{4}$	N	[MeV]	n	N
(stat1; )	0.35	700		1					
(stat2; )	0.35	680		1					
(stat; ; ; 0)	0.224	1200		1	20.45	1600		2	0

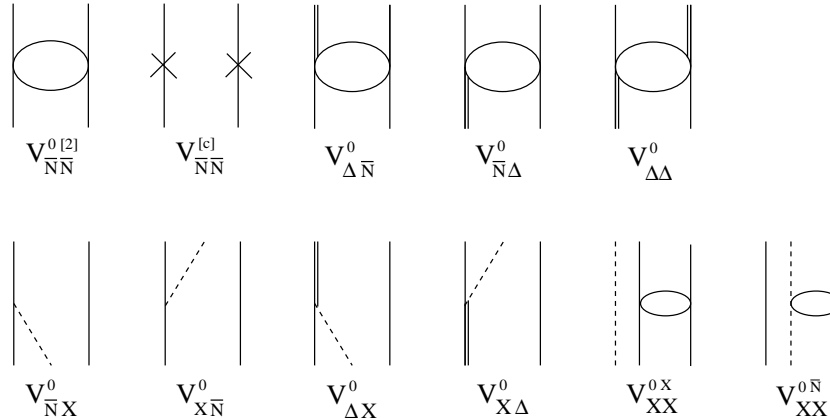


FIG. 1. Diagrammatic representation of the various components of  $V^0$ . The open ellipse symbolizes a given bare mean two-body interaction. The one-nucleon counter term  $v^{[c]}$  is indicated by a cross.

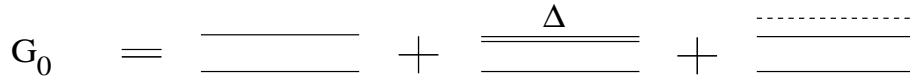


FIG. 2. Diagrammatic representation of the free propagator  $G_0(z)$  with the three contributions in  $H_{NN}^{[2]}$ ,  $H_N^{[2]}$ , and  $H_{X\bar{N}N}^{[2]}$ .

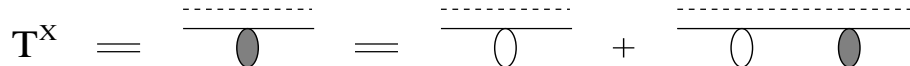


FIG. 3. Diagrammatic representation of the  $N\bar{N}$  scattering matrix  $T^X(z)$  in the presence of a spectator meson.

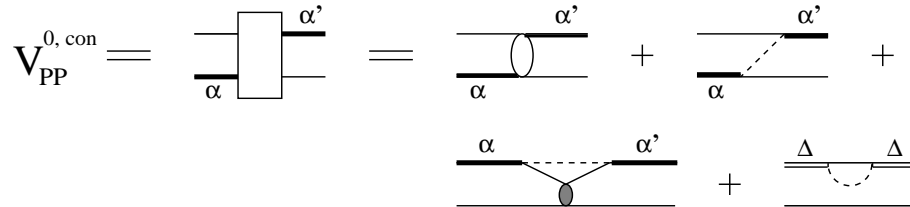


FIG. 4. Diagrammatic representation of the connected driving term  $V_{PP}^{0, con}(z)$ . The greek letters  $\alpha$  and  $\alpha'$  label either a bare nucleon  $N$  or a  $\bar{N}$ .

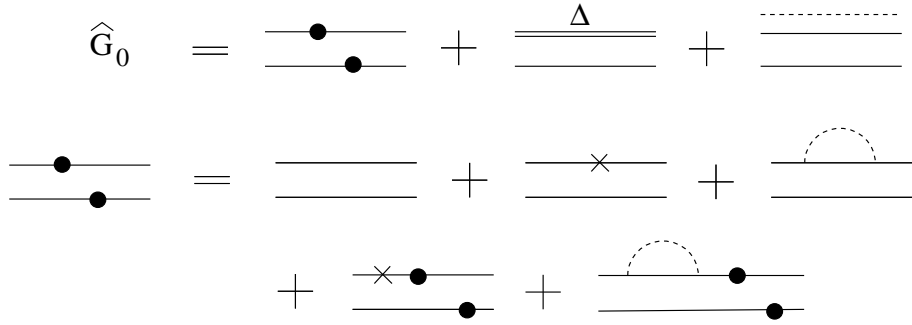


FIG. 5. Diagrammatic representation of the dressed propagator  $\hat{G}_0(z)$ . The cross represents the one-nucleon counter term  $v^{[c]}$ .

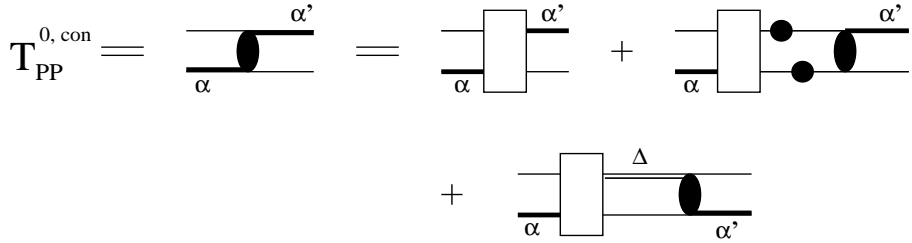


FIG. 6. Graphical representation of the scattering amplitude  $T_{PP}^{0,con}(z)$ . The greek letters  $\alpha$  and  $\alpha'$  label either a bare nucleon  $N$  or a  $\pi$ . The driving term  $V_{PP}^{0,con}(z)$  is shown in Fig. 4.

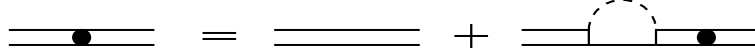


FIG. 7. Diagrammatic representation of the dressed propagator  $g$  (see Eq. (136)). In order to distinguish  $g$  from the free propagator, it is denoted by a \".

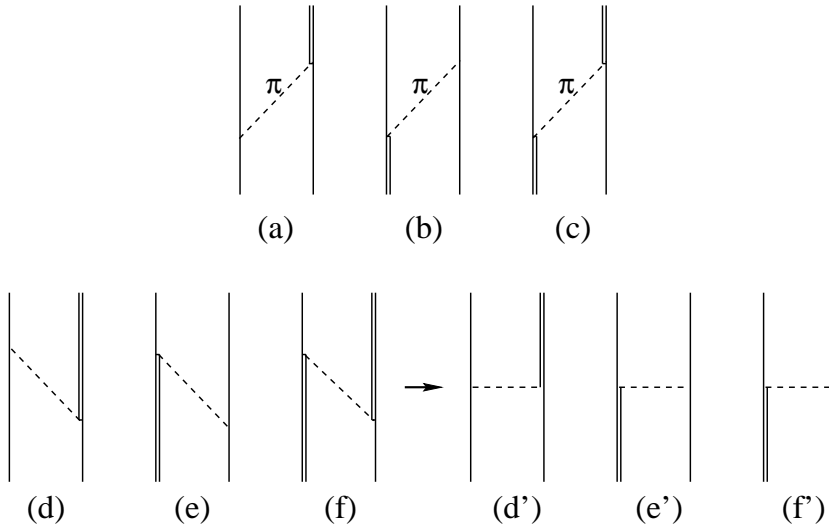


FIG. 8. One-boson exchange diagrams for the various interactions involving a  $N$  configuration. Diagrams (a) through (c) represent retarded contributions (here only). Diagrams (d) through (f) are treated in the energy independent approximation as indicated by the diagrams (d') through (f') because of the absence of  $N$  and  $\pi$  configurations.

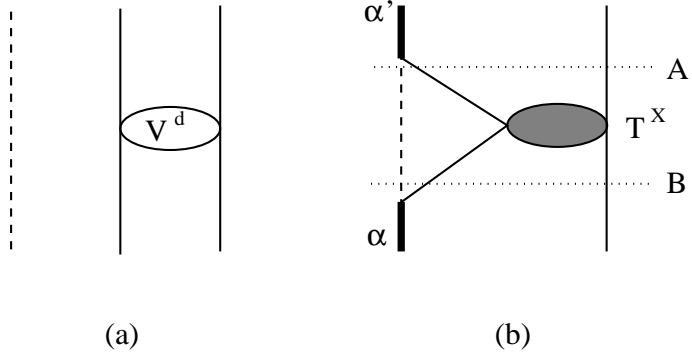


FIG. 9. (a) Diagrammatic representation of  $V_{X_X}^0$  describing the interaction  $V_{N_N}^d$  between the two nucleons in the  $^3S_1 - ^3D_1$  channel with a pion as spectator; (b) Diagrammatic representation of the term  $V_{P_X}^0 G_0(z) T^X(z) G_0(z) V_{X_P}^0$  given in Eq. (65).

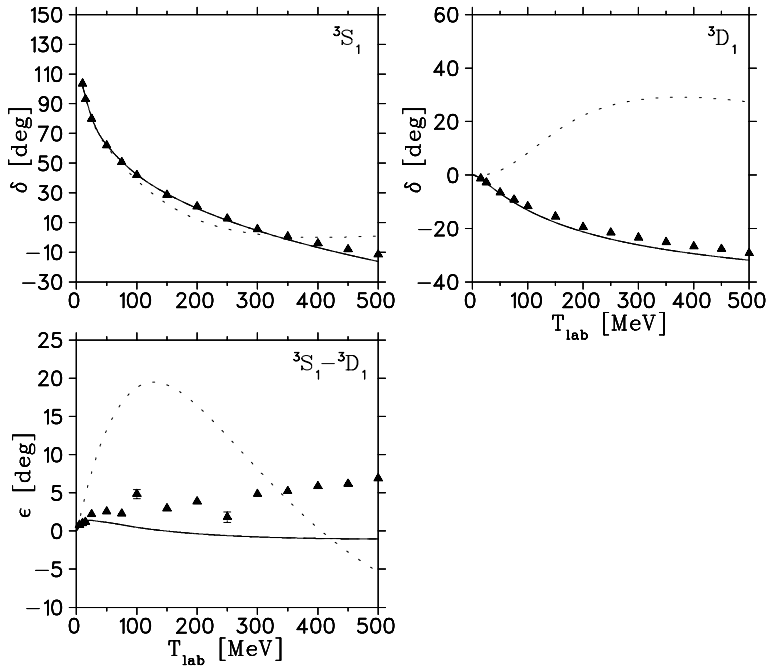


FIG. 10. Phase shifts and mixing angle for the  $^3S_1 - ^3D_1$  channel as a function of the kinetic energy  $T_{\text{lab}}$  of the nucleon in the laboratory system, compared with the experimental data (solution SM 97 of Arndt et al. [31]). For the interaction  $V^d$  in Eq. (161) we have used: dotted: separable ansatz (162) with the deuteron wave function of the Bonn OBEPF potential; solid: exact calculation using the full OBEPF potential.

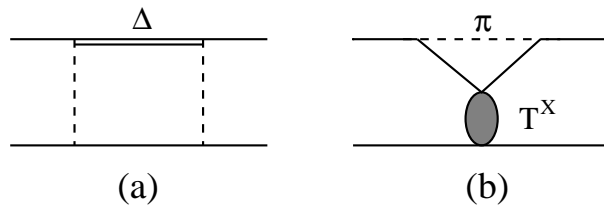


FIG. 11. Dispersive contributions to the NN interaction, which have to be eliminated by renormalization from a realistic nucleon-nucleon potential: (a) from intermediate N states, (b) from intermediate off shell NN scattering in the presence of a spectator meson.

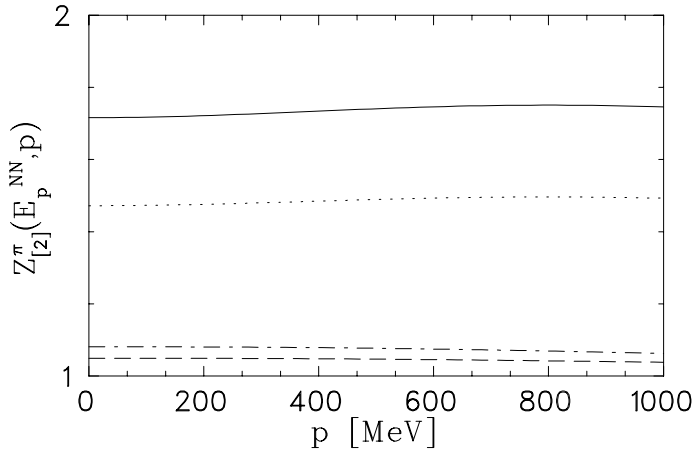


FIG. 12. The renormalization factor  $Z_{[2]}(E_p^{NN}, p)$  of Eq. (180) as function of the external nucleon momentum  $p$  for different parameter sets: dashed:  $\frac{(g^0)^2}{4} = 15, \quad = 500$  MeV; dash-dotted:  $\frac{(g^0)^2}{4} = 15, \quad = 1700$  MeV; dotted:  $\frac{(g^0)^2}{4} = 25, \quad = 500$  MeV; solid:  $\frac{(g^0)^2}{4} = 25, \quad = 1700$  MeV. A dipole form factor has been used.

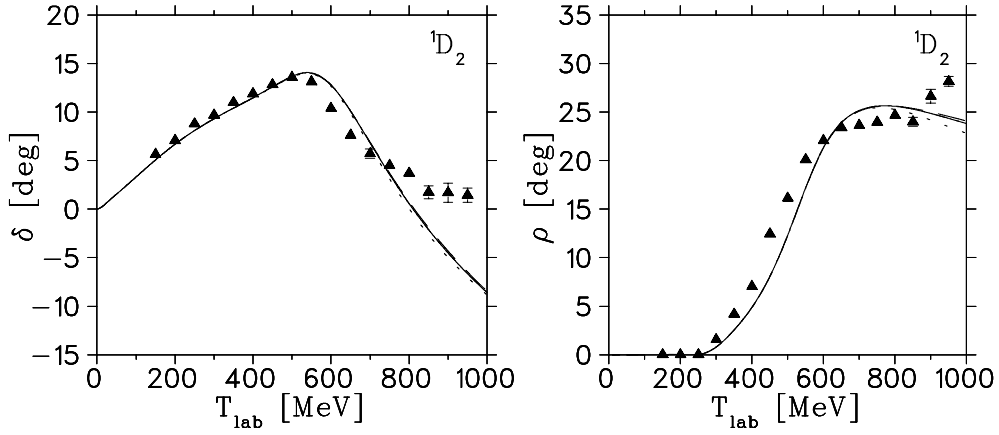


FIG. 13. Phase shift and inelasticity for the  $^1D_2$  channel in comparison with experiment (solution SM 97 of Amdt et al. [31]) for different retarded potential models (see Table III): full curve: CC (ret; ; 0), dotted curve: CC (ret; ; 1), and dashed curve: CC (ret; ; -1).

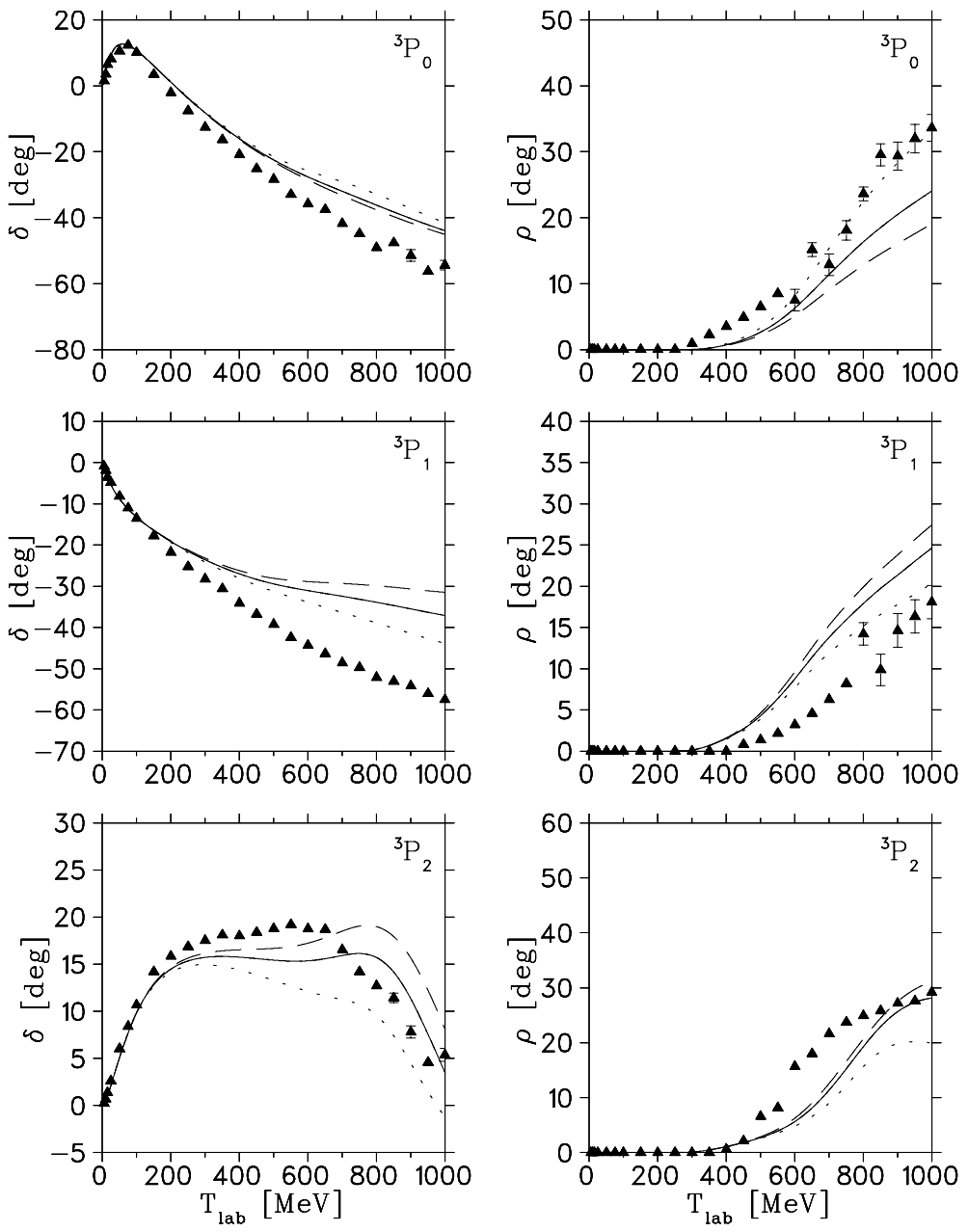


FIG. 14. Phase shift and inelasticity for the  $^3P_0$ ,  $^3P_1$ , and  $^3P_2$  channels. Experimental data and notation of the curves as in Fig. 13.

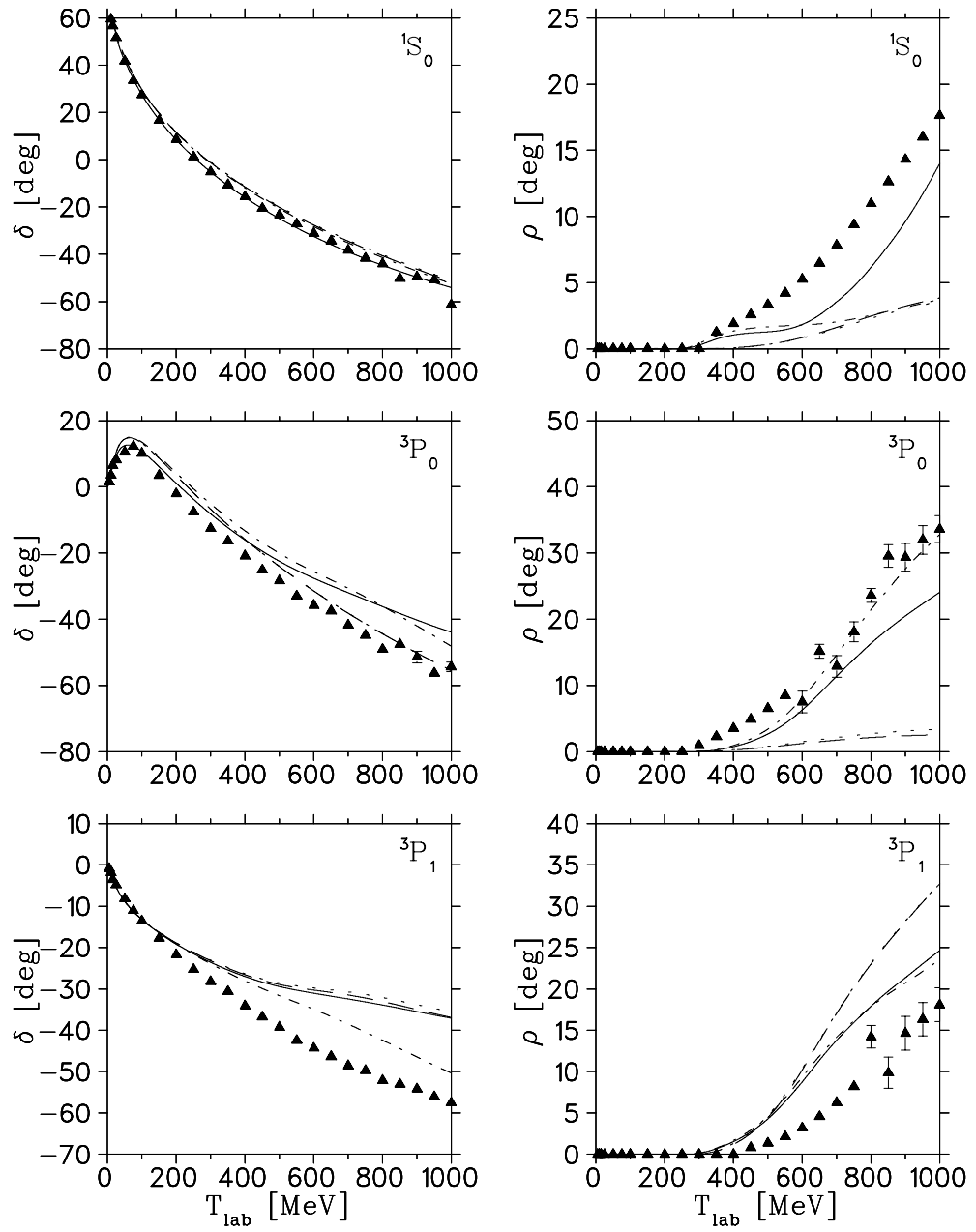


FIG. 15. Phase shift and inelasticity for the  $^1S_0$ ,  $^3P_0$  and  $^3P_1$  channels: dotted curve: CC (stat1; -), dashed curve: CC (stat2; -), dash-dotted curve: CC (stat; ; 0), and full curve: CC (ret; ; 0). The experimental data represent solution SM 97 of Amndt et al. [31].

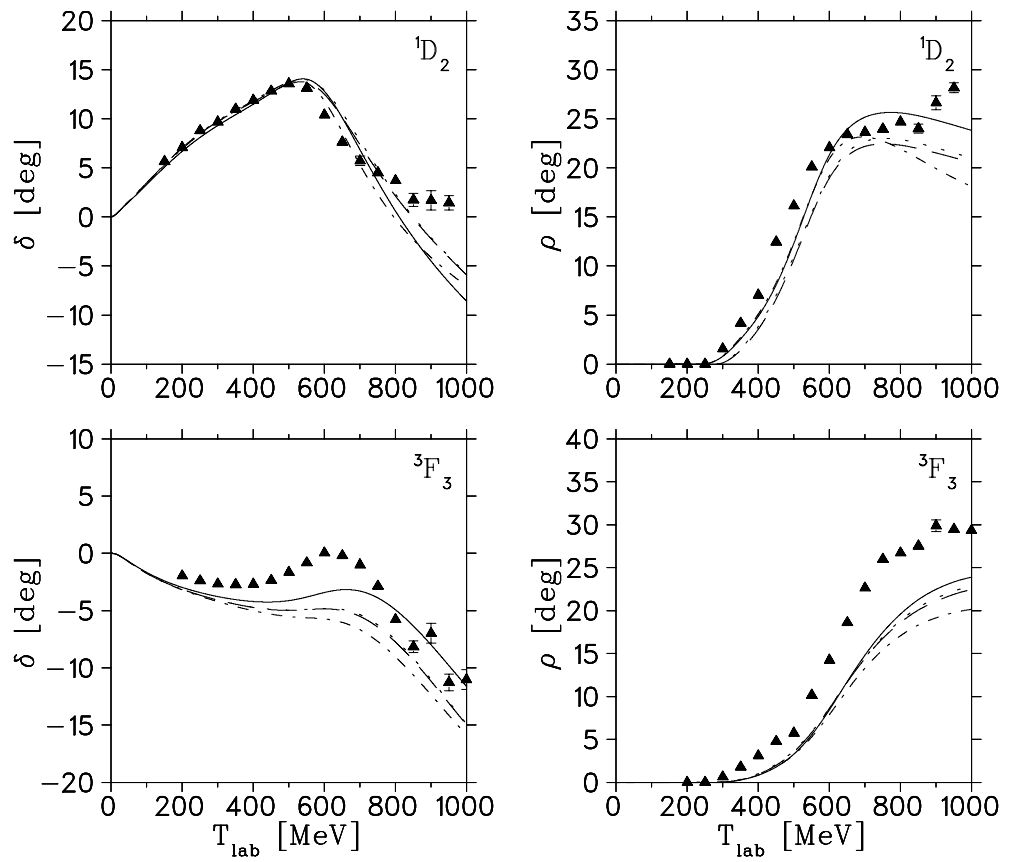


FIG. 16. Phase shift and inelasticity for the  $^1D_2$  and  $^3F_3$  channels. Experimental data and notation of the curves as in Fig. 15.

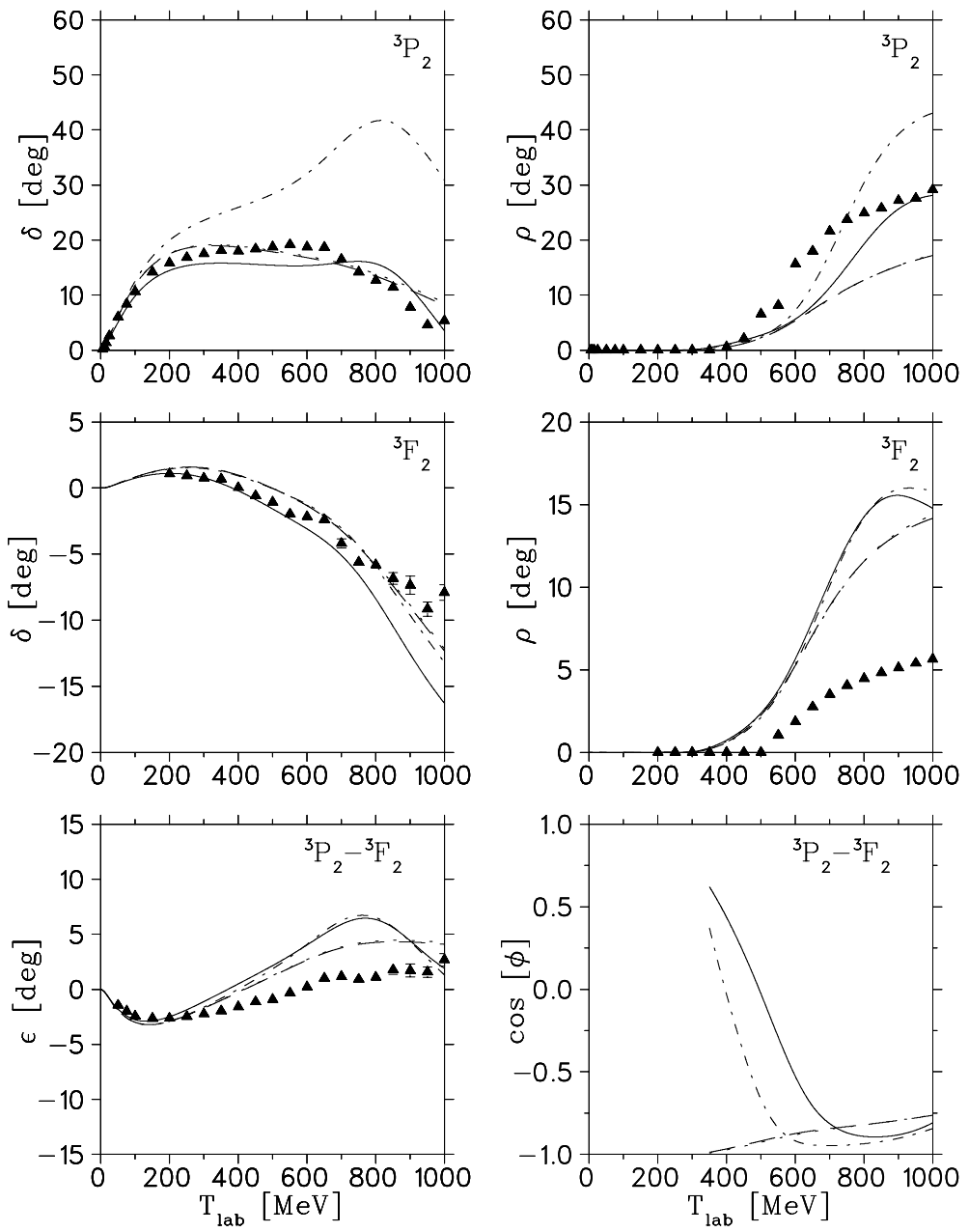


FIG. 17. Phase shifts, inelasticities and mixing angles for the  $^3P_2 - ^3F_2$  channel. Experimental data and notation of the curves as in Fig. 15.